Flight Dynamics Model for the Real-Time Flight Simulation

Zielonka 2019

Author: Marek M. Cel

Revision: 3

Date: 2019-08-04

Statement of Purpose

The laws of most jurisdictions throughout the world automatically confer exclusive Copyright and Related Rights (defined below) upon the creator and subsequent owner(s) (each and all, an "owner") of an original work of authorship and/or a database (each, a "Work").

Certain owners wish to permanently relinquish those rights to a Work for the purpose of contributing to a commons of creative, cultural and scientific works ("Commons") that the public can reliably and without fear of later claims of infringement build upon, modify, incorporate in other works, reuse and redistribute as freely as possible in any form whatsoever and for any purposes, including without limitation commercial purposes. These owners may contribute to the Commons to promote the ideal of a free culture and the further production of creative, cultural and scientific works, or to gain reputation or greater distribution for their Work in part through the use and efforts of others.

For these and/or other purposes and motivations, and without any expectation of additional consideration or compensation, the person associating CC0 with a Work (the "Affirmer"), to the extent that he or she is an owner of Copyright and Related Rights in the Work, voluntarily elects to apply CC0 to the Work and publicly distribute the Work under its terms, with knowledge of his or her Copyright and Related Rights in the Work and the meaning and intended legal effect of CC0 on those rights.

1. Copyright and Related Rights. A Work made available under CC0 may be protected by copyright and related or neighboring rights ("Copyright and Related Rights"). Copyright and Related Rights include, but are not limited to, the following:

i. the right to reproduce, adapt, distribute, perform, display, communicate, and translate a Work;
ii. moral rights retained by the original author(s) and/or performer(s);
iii. publicity and privacy rights pertaining to a person's image or likeness depicted in a Work;
iv. rights protecting against unfair competition in regards to a Work, subject to the limitations in paragraph 4(a), below;

v. rights protecting the extraction, dissemination, use and reuse of data in a Work;

vi. database rights (such as those arising under Directive 96/9/EC of the European Parliament and of the Council of 11 March 1996 on the legal protection of databases, and under any national implementation thereof, including any amended or successor version of such directive); and

vii. other similar, equivalent or corresponding rights throughout the world based on applicable law or treaty, and any national implementations thereof.

2. Waiver. To the greatest extent permitted by, but not in contravention of, applicable law, Affirmer hereby overtly, fully, permanently, irrevocably and unconditionally waives, abandons, and surrenders all of Affirmer's Copyright and Related Rights and associated claims and causes of action, whether now known or unknown (including existing as well as future claims and causes of action), in the Work (i) in all territories worldwide, (ii) for the maximum duration provided by applicable law or treaty (including future time extensions), (iii) in any current or future medium and for any number of copies, and (iv) for any purpose whatsoever, including without limitation commercial, advertising or promotional purposes (the "Waiver"). Affirmer makes the Waiver for the benefit of each member of the public at large and to the detriment of Affirmer's heirs and successors, fully intending that such Waiver shall not be subject to revocation, rescission, cancellation, termination, or any other legal or equitable action to disrupt the quiet enjoyment of the Work by the public as contemplated by Affirmer's express Statement of Purpose.

3. Public License Fallback. Should any part of the Waiver for any reason be judged legally invalid or ineffective under applicable law, then the Waiver shall be preserved to the maximum extent permitted taking into account Affirmer's express Statement of Purpose. In addition, to the extent the Waiver is so judged Affirmer hereby grants to each affected person a royalty-free, non transferable, non sublicensable, non exclusive, irrevocable and unconditional license to exercise Affirmer's Copyright and Related Rights in the Work (i) in all territories worldwide, (ii) for the maximum duration provided by applicable law or treaty (including future time extensions), (iii) in any current or future medium and for any number of copies, and (iv) for any purpose whatsoever, including without limitation commercial, advertising or promotional purposes (the "License"). The License shall be deemed effective as of the date CC0 was applied by Affirmer to the Work. Should any part of the License for any reason be judged legally invalid or ineffective under applicable law, such partial invalidity or ineffectiveness shall not invalidate the remainder of the License, and in such case Affirmer hereby affirms that he or she will not (i) exercise any of his or her remaining Copyright and Related Rights in the Work or (ii) assert any associated claims and causes of action with respect to the Work, in either case contrary to Affirmer's express Statement of Purpose.

4. Limitations and Disclaimers.

a. No trademark or patent rights held by Affirmer are waived, abandoned, surrendered, licensed or otherwise affected by this document.
b. Affirmer offers the Work as-is and makes no representations or warranties of any kind concerning the Work, express, implied, statutory or otherwise, including without limitation warranties of title, merchantability, fitness for a particular purpose, non infringement, or the absence of latent or other defects, accuracy, or the present or absence of errors, whether or not discoverable, all to the greatest extent permissible under applicable law.
c. Affirmer disclaims responsibility for clearing rights of other persons that may apply to the Work or any use thereof, including without limitation any person's Copyright and Related Rights in the Work. Further, Affirmer disclaims responsibility for obtaining any necessary consents, permissions or other rights required for any use of the Work.
d. Affirmer understands and acknowledges that Creative Commons is not a party to this document and has no duty or obligation with respect to this CC0 or use of the Work.

Table of Contents

Notation

$a=\frac{dC_Z}{d\alpha}$, $a=\frac{dC_L}{d\alpha}$	–	[1/rad] lift curve slope
$A_R=\pi R^2$	–	[m^2] rotor disc area
b	–	[m] wing span
B	–	[-] blade tip loss factor
c	–	[N/(m/s)] damping coefficient
c_B	–	[m] rotor blade chord
c_{root}	–	[m] chord at wing root
c_{tip}	–	[m] chord at wing tip
c_S	–	[m/s] speed of sound
$\hat{c}$	–	[m] mean aerodynamic chord
C_l	–	[-] rolling moment coefficient
C_m	–	[-] pitching moment coefficient
C_n	–	[-] yawing moment coefficient
C_P	–	[-] power coefficient
C_T	–	[-] thrust coefficient
C_X , C_D	–	[-] drag coefficient
C_Y	–	[-] side force coefficient
C_Z , C_L	–	[-] lift coefficient
C_μ	–	[-] k-ε turbulence model constant
D	–	[N] drag
D	–	[m] propeller diameter
e	–	[m] flapping hinge offset
g	–	[m/s^2] gravitational acceleration
h	–	[m] altitude
$\vec{H}=\left[H_X, H_Y, H_Z\right]^T$	–	[kg·m^2/s] angular momentum vector
i	–	[rad] incidence angle
I	–	[-] turbulence intensity
I_B	–	[kg·m^2] rotor blade moment of inertia
$\boldsymbol{I}$	–	[kg·m^2] inertia matrix
J	–	[-] propeller advance ratio
k	–	[N/m] spring constant
k	–	[m^2/s^2] turbulence kinetic energy
k	–	[-] gain
L	–	[N] lift
L	–	[m] reference length scale
m	–	[kg] mass
$\boldsymbol{M}$	–	[kg],[kg·m],[kg·m^2] generalized inertia matrix
n	–	[rev/s] propeller revolution speed
N_B	–	number of rotor blades
p	–	[Pa] pressure
P	–	[W] power

$\vec{P}=\left[P_X, P_Y, P_Z\right]^T$ – [kg·m/s] momentum vector
Q – [N·m] torque
$\vec{Q}=\left[L, M, N\right]^T$ – [N·m] moment of force vector
r – [m] coordinate along blade span
$\vec{r}=\left[x, y, z\right]^T$ – [m] coordinates vector
R – [N·m/(kmol·K)] universal gas constant
R – [m] rotor radius
$\vec{R}=\left[X, Y, Z\right]^T$ – [N] force vector
Re – [-] Reynolds number
s – [-] complex variable
$s=\frac{N_B c_B}{\pi R}$ – [-] rotor solidity
$\boldsymbol{s}=\left[u, v, w, p, q, r\right]^T$ – [m/s],[rad/s] aircraft state vector expressed in BAS
S – [m^2] wing area
S – [K] Sutherland constant
S_B – [kg·m] blade first moment of mass about flapping hinge
$\vec{S}=\left[S_X, S_Y, S_Z\right]^T$ – [kg·m] first moment of mass
t – [s] time variable
T – [K] temperature
T – [N] thrust
T – [s] time constant
V – [m/s] velocity
V_I – [m/s] induced velocity
V_{IH} – [m/s] induced velocity for hovering
$\vec{V}=\left[u, v, w\right]^T$ – [m/s] velocity vector
$\boldsymbol{x}=\left[x, y, z, e_0, e_X, e_Y, e_Z\right]^T$ – [m],[-] aircraft coordinates vector expressed in WGS-84
α – [rad] angle of attack
β – [rad] angle of sideslip
β – [rad] rotor blade flapping angle
β_0 – [rad] rotor coning angle
β_{1c}, β_{1s} – [rad] longitudinal and lateral tip-path plane tilt angle
$\gamma=\frac{\rho a\, c_B R^4}{I_B}$ – [-] blade Lock number
$\hat{\delta}$ – [-] normalized controls position
ε – [rad] rotor shaft inclination angle (positive forward)
θ_0 – [rad] collective pitch angle
θ_{1s}, θ_{1c} – [rad] longitudinal and lateral cyclic pitch angle
Θ – [rad] pitch angle
λ – [rad] geographic longitude
λ – [-] wing taper ratio
$\lambda=\frac{w_{rw}-V_I}{\left(\Omega_R R\right)}$ – [-] rotor inflow ratio

$\lambda_I = \frac{V_I}{(\Omega_R R)}$ – [-] induced inflow ratio

$\lambda_{IH} = \frac{V_{IH}}{(\Omega_R R)}$ – [-] rotor induced inflow ratio for hovering

μ – [-] friction coefficient

μ – [Pa·s] dynamic viscosity

$\mu = \frac{V}{\Omega_R R}$ – [-] rotor advance ratio

$\mu_C = \frac{V_C}{\Omega_R R}$ – [-] normalized climb velocity

$\mu_D = \frac{V_D}{\Omega_R R}$ – [-] normalized descent velocity

ν – [m^2/s] kinematic viscosity

ρ – [kg/m^3] air density

φ – [rad] geographic latitude

Φ – [rad] roll angle

χ – [rad] rotor wake angle

Ψ – [rad] yaw angle

Ψ – [rad] rotor blade azimuth

ω – [1/s] specific turbulence dissipation rate

ω – [Hz] cutoff frequency

$\vec{\Omega} = [p, q, r]^T$ – [rad/s] angular velocity vector

Ω_R – [rad/s] rotor revolution speed

$\frac{\partial \epsilon}{\partial \alpha}$ – [-] horizontal stabilizer downwash angle derivative with respect to the aircraft angle of attack

Indices:

AC – aerodynamic center
a – Aerodynamic Axis System
b – Body Axis System
ba – Blade Axis System
B – rotor blade
c – Control Axis System
cw – Control-Wind Axis System
C – climb
CM – Center of Mass
D – descent
g – Gravity (North-East-Down) Axis System
h – horizontal stabilizer
I – induced
IH – induced in hovering
N – normal
O – coordinate system’s origin
r – Rotor Axis System
rw – Rotor-Wind Axis System
R – rotor

RH – rotor hub
s – Stability Axis System
T – tangent
v – vertical stabilizer
X – x-axis component
Y – y-axis component
Z – z-axis component

Derivatives:

$\dot{u}=\frac{du}{dt}$ – time derivative
$\bar{\beta}=\frac{d\beta}{d\Psi}$ – azimuth derivative

1. Introduction

1.1. Conventions

Flight Dynamics Model uses International System of Units (SI) for all internal computations. It is clearly specified if other units are used.

All rotations and rotation related operations are considered to be a passive (alias) rotations.

1.2. Coordinates Systems

1.2.1. Body Axis System

Body Axis System is body-centered, body-fixed coordinate system, with the x-axis positive forwards, the y-axis positive right and the z-axis positive downwards.

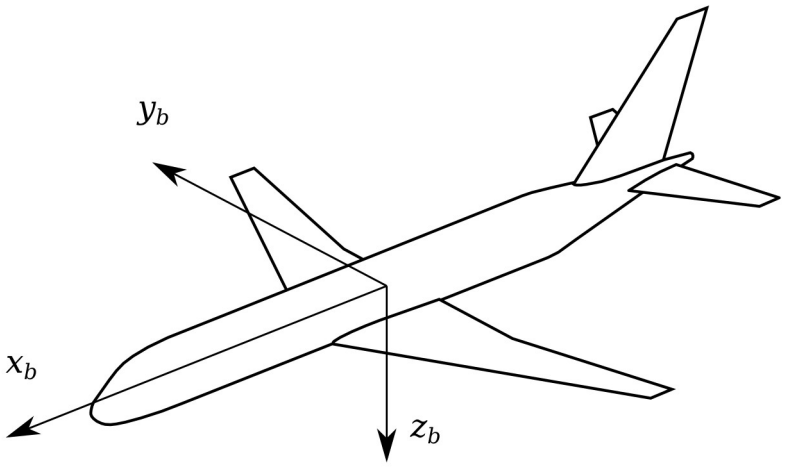

Figure 1-1: Body Axis System

1.2.2. Stability Axis System

Origin of the Stability Axis System is coincident with the origin of the Body Axis System, the x-axis is directed along air freestream velocity vector projected onto the XZ plane of the Body Axis System, the y-axis is coincident with the the y-axis of the Body Axis System, and the z-axis completes a right-handed coordinate system.

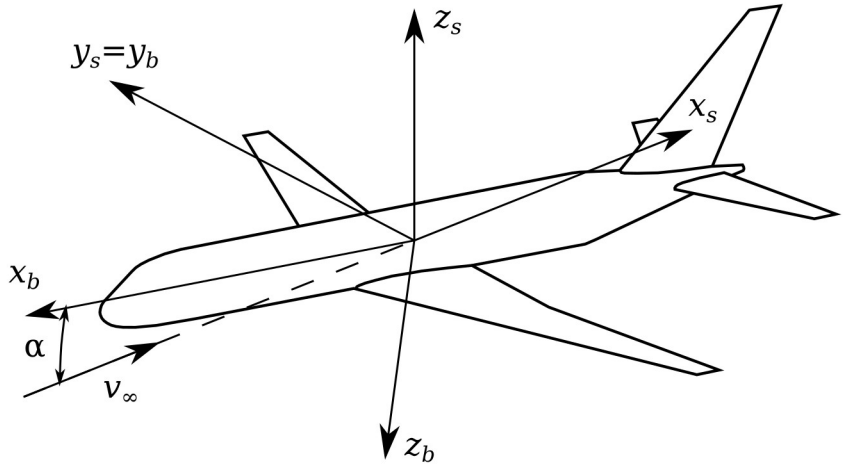

Figure 1-2: Stability Axis System

1.2.3. Aerodynamic Axis System

Origin of the Aerodynamic Axis System is coincident with the origin of the Body Axis System, the x-axis is directed along air freestream velocity vector, the z-axis lies in the aircraft plane of symmetry pointing upwards, and the y-axis completes a right-handed coordinate system.

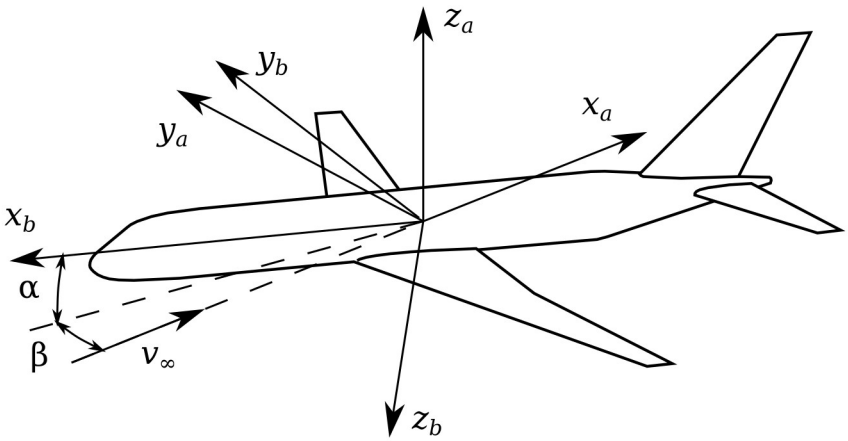

Figure 1-3: Aerodynamic Axis System

1.2.4. Gravity Axis System

There are basically two conventions of Gravity Axis Systems used for the purpose of flight dynamics East-North-Up and North-East-Down.

It is convenient to use North-East-Down axes system together with the Body Axis System and Bryant angles (Euler angles in z-y-x convention) as those angles in NED frame become aircraft heading, pitch and roll.

Considering all this, Gravity Earth Axis System is a coordinate system, with the x-axis positive North, the y-axis positive East and z-axis positive downwards.

1.2.5. Earth-fixed Axis System

For any further considerations World Geodetic System 1984 as described in [1] is used as the Earth-fixed Axis System.

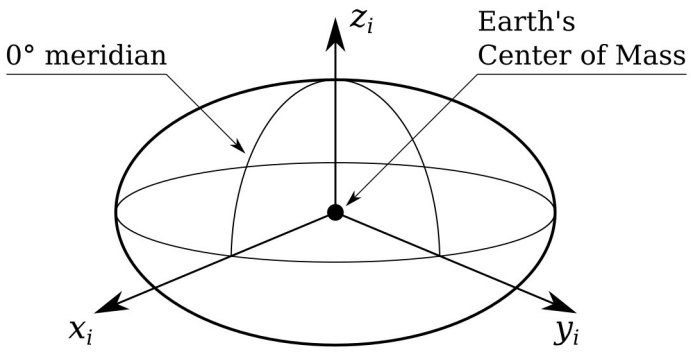

Figure 1-4: World Geodetic System 1984

1.3. Aircraft Attitude

Aircraft attitude is defined either by a quaternion or by quasi-Euler Tait-Bryan ψ-θ-φ angles in z-y-x convention. It is convenient to use such a convention, as this angles becomes aircraft roll, pitch and heading when expressed in North-East-Down coordinate system.

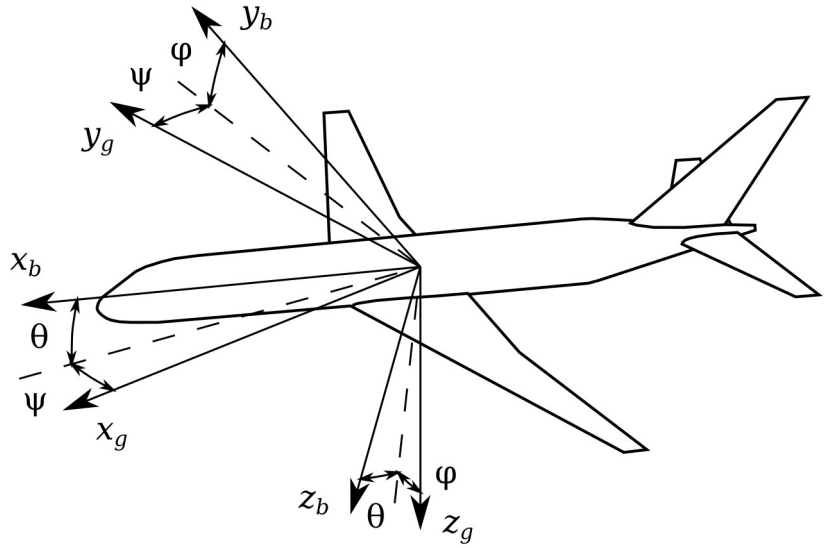

Figure 1-5: Tait–Bryan angles

1.4. Transformations Between Coordinates Systems

1.4.1. Rotation Matrices

Transformation to the coordinate system rotated by Tait-Bryan Ψ-Θ-Φ angles can be performed using rotation matrix, which is given by the following relations. [2, 3]

$$\boldsymbol{T}(\Phi)=\begin{bmatrix}1 & 0 & 0\\ 0 & \cos\Phi & \sin\Phi\\ 0 & -\sin\Phi & \cos\Phi\end{bmatrix} \tag{1.1}$$

$$\boldsymbol{T}(\Theta)=\begin{bmatrix}\cos\Theta & 0 & -\sin\Theta\\ 0 & 1 & 0\\ \sin\Theta & 0 & \cos\Theta\end{bmatrix} \tag{1.2}$$

$$\boldsymbol{T}(\Psi)=\begin{bmatrix}\cos\Psi & \sin\Psi & 0\\ -\sin\Psi & \cos\Psi & 0\\ 0 & 0 & 1\end{bmatrix} \tag{1.3}$$

$$\begin{aligned}\boldsymbol{T}(\Phi,\Theta,\Psi)&=\boldsymbol{T}(\Phi)\boldsymbol{T}(\Theta)\boldsymbol{T}(\Psi)=\\ &=\begin{bmatrix}\cos\Theta\cos\Psi & \cos\Theta\sin\Psi & -\sin\Theta\\ \cos\Psi\sin\Phi\sin\Theta-\cos\Phi\sin\Psi & \cos\Phi\cos\Psi+\sin\Phi\sin\Theta\sin\Psi & \cos\Theta\sin\Phi\\ \sin\Phi\sin\Psi+\cos\Phi\cos\Psi\sin\Theta & \cos\Phi\sin\Theta\sin\Psi-\cos\Psi\sin\Phi & \cos\Phi\cos\Theta\end{bmatrix}\end{aligned} \tag{1.4}$$

1.4.2. Geographic Coordinates

Conversion from Geographic to Cartesian Coordinates

Procedure of conversion from geographic coordinates to the Cartesian coordinates system is given as follows.

$$e=\frac{1}{a}\sqrt{a^2-b^2} \tag{1.5}$$

$$\chi=\sqrt{1-e^2\sin^2\varphi} \tag{1.6}$$

$$x_i=\left(\frac{a}{\chi}+h\right)\cos\varphi\cos\lambda \tag{1.7}$$

$$y_i=\left(\frac{a}{\chi}+h\right)\cos\varphi\sin\lambda \tag{1.8}$$

$$z_i=\left(a\frac{1-e^2}{\chi}+h\right)\sin\varphi \tag{1.9}$$

Conversion from Cartesian to Geographic Coordinates

Reverse conversion is given as follows. [4]

$$r=\sqrt{x_i^2+y_i^2} \tag{1.10}$$

$$E^2=a^2-b^2 \tag{1.11}$$

$$e'^2=\frac{a^2-b^2}{b^2} \tag{1.12}$$

$$F=54\,b^2 z_i^2 \tag{1.13}$$

$$G=r^2+\left(1-e^2\right)z_i^2-e^2E^2 \tag{1.14}$$

$$C=\frac{e^4 F r^2}{G^3} \tag{1.15}$$

$$S=\sqrt[3]{1+C+\sqrt{C^2+2C}} \tag{1.16}$$

$$P_0=S+\frac{1}{S}+1 \tag{1.17}$$

$$P=\frac{F}{3P_0^2G^2} \tag{1.18}$$

$$Q=\sqrt{1+2e^4P} \tag{1.19}$$

$$r_0=\frac{-\left(Pe^2r\right)}{1+Q}+\sqrt{\frac{1}{2}a^2\left(1+\frac{1}{Q}\right)-\frac{P\left(1-e^2\right)z_i^2}{Q+Q^2}-\frac{1}{2}Pr^2} \tag{1.20}$$

$$U_0=r-e^2r_0 \tag{1.21}$$

$$U=\sqrt{U_0^2+z_i^2} \tag{1.22}$$

$$V=\sqrt{U_0^2+\left(1-e^2\right)z_i^2} \tag{1.23}$$

$$Z_0=\frac{b^2z_i}{aV} \tag{1.24}$$

$$h=U\left(1-\frac{b^2}{aV}\right) \tag{1.25}$$

$$\varphi=\arctan\left(\frac{z_i+e'^2Z_0}{r}\right) \tag{1.26}$$

$$\lambda=\arctan\left(\frac{y_i}{x_i}\right) \tag{1.27}$$

where

a – [m] equatorial radius (6,378,137 m [1])

b – [m] polar radius (6,356,752.3142 m [1])

h – [m] altitude

λ – [rad] geographic longitude

φ – [rad] geographic latitude

2. Flight Dynamics Model

2.1. Assumptions

Following assumptions are made:

– forces and moments acting on the aircraft are considered to be quasi-steady,

– aircraft is considered to be a rigid body,

– mass and moments of inertia depend only on variable masses (fuel, payload, etc.).

2.2. Equations of Motion

2.2.1. Dynamic Equations

Dynamic equations of motion are derived in Body Axis System for a rigid aircraft using conservation of momentum and angular momentum principles which are given by the following formulas. [5, 6, 7]

$$\frac{d\vec{P}_b}{dt}=\sum_{j=1}\vec{R}_{j,b} \tag{2.1}$$

$$\frac{d\vec{H}_{O,b}}{dt}+\vec{V}_{O,b}\times\vec{P}_b=\sum_{j=1}\vec{Q}_{O,j,b} \tag{2.2}$$

where

$$\sum_{j=1}\vec{R}_{j,b}=\vec{R}_{A,b}+\vec{R}_{M,b}+\vec{R}_{LG,b}+\vec{R}_{P,b} \tag{2.3}$$

$$\sum_{j=1}\vec{Q}_{O,j,b}=\vec{Q}_{O,A,b}+\vec{Q}_{O,M,b}+\vec{Q}_{O,LG,b}+\vec{Q}_{O,P,b} \tag{2.4}$$

Momentum and angular momentum are [6, 7]

$$\vec{P}_b=m\vec{V}_{CM,b} \tag{2.5}$$

$$\vec{H}_{O,b}=\boldsymbol{I}_{O,b}\vec{\Omega}_b+m\left(\vec{r}_{CM,b}\times\vec{V}_{O,b}\right) \tag{2.6}$$

Center of mass velocity is

$$\vec{V}_{CM,b}=\vec{V}_{O,b}+\vec{\Omega}_b\times\vec{r}_{CM,b} \tag{2.7}$$

Substituting equation (2.7) into equations (2.5) and (2.6) gives

$$\vec{P}_b = m\left[\vec{V}_O\right]_b + \vec{\Omega}_b \times \vec{S}_b \tag{2.8}$$

$$\vec{H}_{O,b} = \boldsymbol{I}_b \vec{\Omega}_b + \vec{S}_b \times \vec{V}_{O,b} \tag{2.9}$$

where

$$\vec{S}_b = \left[S_X, S_Y, S_Z\right]^T = m\vec{r}_{CM,b} \tag{2.10}$$

Derivatives of momentum and angular momentum in rotating reference frame are [5, 6, 7]

$$\frac{d\vec{P}_b}{dt} = \frac{\delta \vec{P}_b}{\delta t} + \vec{\Omega}_b \times \vec{P}_b \tag{2.11}$$

$$\frac{d\vec{H}_{O,b}}{dt} = \frac{\delta \vec{H}_{O,b}}{\delta t} + \vec{\Omega}_b \times \vec{H}_{O,b} \tag{2.12}$$

Substituting equations (2.11) and (2.12) into (2.1) and (2.2) gives

$$\frac{\delta \vec{P}_b}{\delta t} = \sum_j \vec{R}_{j,b} - \vec{\Omega}_b \times \vec{P}_b \tag{2.13}$$

$$\frac{\delta \vec{H}_{O,b}}{\delta t} = \sum_j \vec{Q}_{O,j,b} - \vec{V}_{O,b} \times \vec{P}_b - \vec{\Omega}_b \times \vec{H}_{O,b} \tag{2.14}$$

Differentiating equations (2.8) and (2.9) gives

$$\frac{\delta \vec{P}_b}{\delta t} = m\frac{\delta \vec{V}_{O,b}}{\delta t} + \frac{\delta \vec{\Omega}_b}{\delta t} \times \vec{S}_b \tag{2.15}$$

$$\frac{\delta \vec{H}_{O,b}}{\delta t} = \boldsymbol{I}_b \frac{\delta \vec{\Omega}_b}{\delta t} + \vec{S}_b \times \frac{\delta \vec{V}_{O,b}}{\delta t} \tag{2.16}$$

Substituting equations (2.15) and (2.16) into (2.13) and (2.14) gives

$$m\frac{\delta \vec{V}_{O,b}}{\delta t} + \frac{\delta \vec{\Omega}_b}{\delta t} \times \vec{S}_b = \sum_j \vec{R}_{j,b} - \vec{\Omega}_b \times \vec{P}_b \tag{2.17}$$

$$\boldsymbol{I}_b \frac{\delta \vec{\Omega}_b}{\delta t} + \vec{S}_b \times \frac{\delta \vec{V}_{O,b}}{\delta t} = \sum_j \vec{Q}_{O,j,b} - \vec{V}_{O,b} \times \vec{P}_b - \vec{\Omega}_b \times \vec{H}_{O,b} \tag{2.18}$$

Representing vector cross product as matrix-vector multiplication equations (2.17) and (2.18) can be written as

$$\begin{bmatrix} m & 0 & 0 \\ 0 & m & 0 \\ 0 & 0 & m \end{bmatrix}\begin{bmatrix} \dot{u} \\ \dot{v} \\ \dot{w} \end{bmatrix}+\begin{bmatrix} 0 & S_Z & -S_Y \\ -S_Z & 0 & S_X \\ S_Y & -S_X & 0 \end{bmatrix}\begin{bmatrix} \dot{p} \\ \dot{q} \\ \dot{r} \end{bmatrix}=\sum_j \vec{R}_{j,b}-\vec{\Omega}_b\times\vec{P}_b \tag{2.19}$$

$$\begin{bmatrix} I_X & -I_{XY} & -I_{XZ} \\ -I_{XY} & I_Y & -I_{YZ} \\ -I_{XZ} & -I_{YZ} & I_Z \end{bmatrix}\begin{bmatrix} \dot{p} \\ \dot{q} \\ \dot{r} \end{bmatrix}+\begin{bmatrix} 0 & -S_Z & S_Y \\ S_Z & 0 & -S_X \\ -S_Y & S_X & 0 \end{bmatrix}\begin{bmatrix} \dot{u} \\ \dot{v} \\ \dot{w} \end{bmatrix}=\sum_j \vec{Q}_{O,j,b}-\vec{V}_{O,b}\times\vec{P}_b-\vec{\Omega}_b\times\vec{H}_{O,b} \tag{2.20}$$

Combined equations (2.19) and (2.20) can be written as follows. [3]

$$\boldsymbol{M}\,\dot{\boldsymbol{s}}=\boldsymbol{R} \tag{2.21}$$

where

$$\dot{\boldsymbol{s}}=\left[\dot{u},\dot{v},\dot{w},\dot{p},\dot{q},\dot{r}\right]^T \tag{2.22}$$

$$\boldsymbol{R}=\begin{bmatrix} \sum_j \vec{R}_{j,b}-\vec{\Omega}_b\times\vec{P}_b \\ \sum_j \vec{Q}_{O,j,b}-\vec{V}_{O,b}\times\vec{P}_b-\vec{\Omega}_b\times\vec{H}_{O,b} \end{bmatrix} \tag{2.23}$$

$$\boldsymbol{M}=\begin{bmatrix} m & 0 & 0 & 0 & S_Z & -S_Y \\ 0 & m & 0 & -S_Z & 0 & S_X \\ 0 & 0 & m & S_Y & -S_X & 0 \\ 0 & -S_Z & S_Y & I_X & -I_{XY} & -I_{XZ} \\ S_Z & 0 & -S_X & -I_{XY} & I_Y & -I_{YZ} \\ -S_Y & S_X & 0 & -I_{XZ} & -I_{YZ} & I_Z \end{bmatrix} \tag{2.24}$$

For the purpose of numerical simulation equation (2.21) can be written in the following form, which is easy to solve with Gaussian methods.

$$\dot{\boldsymbol{s}}=\boldsymbol{M}^{-1}\boldsymbol{R} \tag{2.25}$$

2.2.2. Kinematic Equations

Time Derivatives

Position vector derivative is given as follows. [8]

$$\begin{bmatrix} \dot{x} \\ \dot{y} \\ \dot{z} \end{bmatrix}=\begin{bmatrix} \cos\Theta\cos\Psi & \cos\Psi\sin\Phi\sin\Theta-\cos\Phi\sin\Psi & \sin\Phi\sin\Psi+\cos\Phi\cos\Psi\sin\Theta \\ \cos\Theta\sin\Psi & \cos\Phi\cos\Psi+\sin\Phi\sin\Theta\sin\Psi & \cos\Phi\sin\Theta\sin\Psi-\cos\Psi\sin\Phi \\ -\sin\Theta & \cos\Theta\sin\Phi & \cos\Phi\cos\Theta \end{bmatrix}\begin{bmatrix} u \\ v \\ w \end{bmatrix} \tag{2.26}$$

Tait-Bryan angles derivatives are given as follows. [3, 8]

$$\begin{bmatrix} \dot{\Phi} \\ \dot{\Theta} \\ \dot{\Psi} \end{bmatrix} = \begin{bmatrix} 1 & \sin\Phi\tan\Theta & \cos\Phi\tan\Theta \\ 0 & \cos\Phi & -\sin\Phi \\ 0 & \frac{\sin\Phi}{\cos\Theta} & \frac{\cos\Phi}{\cos\Theta} \end{bmatrix} \begin{bmatrix} p \\ q \\ r \end{bmatrix} \tag{2.27}$$

There are singularities in equation (2.27) for value of $\Theta = \pm 90°$. One method of solving this problem is to use quaternions instead of Tait-Bryan angles to describe aircraft attitude.

Quaternions

Quaternion time derivative is given as follows. [3, 9]

$$\begin{bmatrix} \dot{e}_0 \\ \dot{e}_X \\ \dot{e}_Y \\ \dot{e}_Z \end{bmatrix} = -\frac{1}{2} \begin{bmatrix} 0 & p & q & r \\ -p & 0 & -r & q \\ -q & r & 0 & -p \\ -r & -q & p & 0 \end{bmatrix} \begin{bmatrix} e_0 \\ e_X \\ e_Y \\ e_Z \end{bmatrix} \tag{2.28}$$

2.3. Numerical Integration

State vector $\boldsymbol{s}$ can be calculated by solving initial value problem given by the following expression.

$$\boldsymbol{s}(t_n) = \boldsymbol{s}(t_0) + \int_{t_0}^{t_n} \dot{\boldsymbol{s}}\, dt \tag{2.29}$$

State vector derivative $\dot{\boldsymbol{s}}$ can be calculated using formula (2.25).

Aircraft position and attitude can be calculated by solving initial value problem given as follows.

$$\boldsymbol{x}(t_0 + \Delta t) = \boldsymbol{x}(t_0) + \int_{t_0}^{t_0+\Delta t} \dot{\boldsymbol{x}}\, dt \tag{2.30}$$

where

$$\boldsymbol{x} = \left[x, y, z, e_0, e_X, e_Y, e_Z\right]^T \tag{2.31}$$

Coordinates vector derivative $\dot{\boldsymbol{x}}$ can be calculated using formulas (2.26) and (2.28).

Initial value problems, given by the (2.29) and (2.30) expressions, can be solved using Runge-Kutta 4th-order method which is given as follows. [10, 11, 12]

$$y(t_0 + \Delta t) \approx y(t_0) + \frac{1}{6}\Delta t\left(k_1 + 2k_2 + 2k_3 + k_4\right) \tag{2.32}$$

where

$$k_1 = f\left(t_n, y_n\right) \tag{2.33}$$

$$k_2 = f\left(t_n + \frac{1}{2}\Delta t, y_n + \frac{1}{2}\Delta t\, k_1\right) \tag{2.34}$$

$$k_3 = f\left(t_n + \frac{1}{2}\Delta t, y_n + \frac{1}{2}\Delta t\, k_2\right) \tag{2.35}$$

$$k_4 = f\left(t_n + \Delta t, y_n + \Delta t\, k_3\right) \tag{2.36}$$

2.4. Environment

2.4.1. Atmosphere

US Standard Atmosphere 1976 is used to calculate air temperature, pressure, density, viscosity and speed of sound depending on altitude.

Mean molecular weight is given as follows.

$$M_0 = \frac{\sum_j M_j F_j}{\sum_j F_j} = 28.9645 \tag{2.37}$$

Temperature is given by the following formula. [13]

$$T(h) = T_j + \left(\frac{dT}{dh}\right)_j \left(h - h_j\right) \tag{2.38}$$

Pressure is given as follows. [13]

$$p(h) = p_j \left(\frac{T_j}{T(h)}\right)^{\frac{g M_0}{R\left(\frac{dT}{dh}\right)_j}} \quad \text{for} \quad \left(\frac{dT}{dh}\right)_j \neq 0 \tag{2.39}$$

$$p(h) = p_j e^{\frac{g M_0 \left(h - h_j\right)}{R T_j}} \quad \text{for} \quad \left(\frac{dT}{dh}\right)_j = 0 \tag{2.40}$$

Density is expressed by the following formula. [13]

$$\rho(h) = \frac{p(h) M_0}{R T(h)} \tag{2.41}$$

Speed of sound is given as follows. [13]

$$c_S = \sqrt{\frac{\gamma R T(h)}{M_0}} \tag{2.42}$$

Dynamic viscosity is given by the formula. [13]

$$\mu = \frac{1.458 \cdot 10^{-6} \sqrt{T(h)^3}}{T(h) + S} \tag{2.43}$$

Kinetic viscosity is given as follows. [13]

$$\nu = \frac{\mu}{\rho} \tag{2.44}$$

Altitude h_j **[m]**	**Temperature gradient** $\left(\frac{dT}{dh}\right)_j$ **[K/m]**	**Temperature** T_j **[K]**	**Pressure** p_j **[Pa]**
0	$-6.5 \cdot 10^{-3}$	288.15	101325.0
11,000	0.0	216.65	22632.0
20,000	$1.0 \cdot 10^{-3}$	216.65	5474.8
32,000	$2.8 \cdot 10^{-3}$	228.65	868.01
47,000	0.0	270.65	110.9
51,000	$-2.8 \cdot 10^{-3}$	270.65	66.938
71,000	$-2.0 \cdot 10^{-3}$	214.65	3.9564

Table 2-1: Reference levels [13]

Gas species	**Molecular weight** M_j **[kg/kmol]**	**Fractional volume** F_j **[-]**
Nitrogen	28.0134	0.78084
Oxygen	31.9988	0.209476
Argon	39.948	0.00934
Carbon Dioxide	44.00995	0.000314
Neon	20.183	0.00001818
Helium	4.0026	0.00000524
Krypton	83.8	0.00000114
Xenon	131.3	0.000000087
Methane	16.04303	0.000002
Hydrogen	2.01594	0.0000005

Table 2-2: Molecular weights and fractional volume composition of sea-level dry air [13]

2.5. Aerodynamics

Aerodynamic forces are calculated in Aerodynamic Axis System, while moments are calculated in Stability Axis System. Rotation matrix from Stability Axis System to Body Axis System can be calculated using formula (2.45). Rotation matrix from Aerodynamic Axis System to Body Axis System can be calculated using following formulas.

$$\boldsymbol{T}(\alpha)=\begin{bmatrix}-1 & 0 & 0\\ 0 & 1 & 0\\ 0 & 0 & -1\end{bmatrix}\begin{bmatrix}\cos\alpha & 0 & -\sin\alpha\\ 0 & 1 & 0\\ \sin\alpha & 0 & \cos\alpha\end{bmatrix}=\begin{bmatrix}-\cos\alpha & 0 & \sin\alpha\\ 0 & 1 & 0\\ -\sin\alpha & 0 & -\cos\alpha\end{bmatrix} \tag{2.45}$$

$$\boldsymbol{T}(\beta)=\begin{bmatrix}\cos\beta & \sin\beta & 0\\ -\sin\beta & \cos\beta & 0\\ 0 & 0 & 1\end{bmatrix} \tag{2.46}$$

$$\boldsymbol{T}(\alpha,\beta)=\boldsymbol{T}(\alpha)\boldsymbol{T}(\beta)=\begin{bmatrix}-\cos\alpha\cos\beta & -\cos\alpha\sin\beta & \sin\alpha\\ -\sin\beta & \cos\beta & 0\\ -\sin\alpha\cos\beta & -\sin\alpha\sin\beta & -\cos\alpha\end{bmatrix} \tag{2.47}$$

Considering a no-wind conditions angle of attack and angle of sideslip (positive when the aircraft velocity component along the transverse axis is positive [14]) are given as follows.

$$\alpha=\arctan\left(\frac{w}{\sqrt{u^2+v^2}}\right) \tag{2.48}$$

$$\beta=\arcsin\left(\frac{v}{V}\right) \tag{2.49}$$

2.5.1. Tail-off Aircraft

Tail-off aircraft aerodynamics model is intended to be used in application, e.g. fixed-wing aircrafts, where asymmetric aerodynamic effects, such as autorotation spin or roll damping, are significant.

Forces and moments are calculated for each half-wing to consider asymmetric effects. Half wing aerodynamic center velocity vector used to calculate angle of attack, angle of sideslip as well as forces and moments is given as follows.

$$\vec{V}_{AC}=\vec{V}_O+\vec{\Omega}\times\vec{r}_{AC} \tag{2.50}$$

Forces and moments generated by the half-wing are given as follows. [9]

$$\vec{F}_a=\left[F_{X,a},F_{Y,a},F_{Z,a}\right]^T \tag{2.51}$$

$$\vec{M}_s=\left[M_{X,s},M_{Y,s},M_{Z,s}\right]^T \tag{2.52}$$

where

$$F_{X,a} = \frac{1}{2}\rho V^2 S C_X \tag{2.53}$$

$$F_{Y,a} = \frac{1}{2}\rho V^2 S C_Y \tag{2.54}$$

$$F_{Z,a} = \frac{1}{2}\rho V^2 S C_Z \tag{2.55}$$

$$M_{X,s} = \frac{1}{2}\rho V^2 S \hat{c} C_l \tag{2.56}$$

$$M_{Y,s} = \frac{1}{2}\rho V^2 S \hat{c} C_m \tag{2.57}$$

$$M_{Z,s} = \frac{1}{2}\rho V^2 S \hat{c} C_n \tag{2.58}$$

Forces and moments generated by the half-wing expressed in Body Axis System are given by the following formulas.

$$\vec{F}_b = \boldsymbol{T}(\alpha,\beta)\vec{F}_a \tag{2.59}$$

$$\vec{M}_b = \boldsymbol{T}(\alpha)\vec{M}_s + \vec{r}_{AC,b} \times \vec{F}_b \tag{2.60}$$

2.5.2. Fuselage

Fuselage aerodynamics model is intended to be used in application where asymmetric aerodynamic effects can be neglected, e.g. to model helicopter fuselage. It is very much like, described above, tail-off aircraft model. The main difference is that calculations are performed for whole fuselage unlike the tail-off aircraft where calculations are performed for each half-wing.

2.5.3. Stabilizers

Velocity vector used to calculate stabilizer angle of attack, angle of sideslip as well as forces and moments is calculated using expression (2.50).

Horizontal stabilizer angle of attack is modified due to incidence angle and downwash angle, what can be expressed as follows. [15]

$$\Delta\alpha_h = i_h + \frac{\partial\epsilon}{\partial\alpha}\alpha \tag{2.61}$$

Forces generated by stabilizers are calculated using formulas (2.53), (2.54) and (2.55).

Formula (2.59) can be used to calculate stabilizer generated forces expressed in Body Axis System.

It is assumed that horizontal stabilizer generates only drag and lift, while vertical stabilizer generates only drag and side force. Moments generated by stabilizers comes only from force acting on arm, other moments are neglected.

$$\vec{M}_b = \vec{r}_{AC,b} \times \vec{F}_b \tag{2.62}$$

2.5.4. Helicopter Rotor

Coordinate Systems Used for Rotor Calculations

Rotor Axis System

Origin of the Rotor Axis System is coincident with the rotor hub center, the x-axis is positive forwards, the y-axis is positive right and z-axis is positive downwards and coincident with the rotor shaft axis.

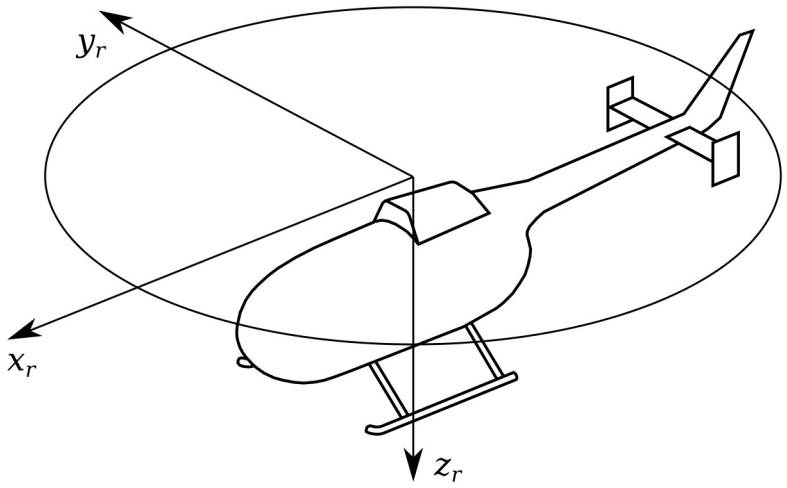

Figure 2-1: Rotor Axis System

Rotor-Wind Axis System

Rotor-Wind Axis System is very much like Rotor Axis System, the only difference is that it is rotated about z-axis in such a manner that x-axis points directly into relative wind, so there is no lateral airspeed component.

Control Axis System

For most purposes, using the Rotor Axis System causes unnecessary complications. It is convenient to use no cyclic feathering axes system. [16] Origin of the Control Axis System is

coincident with the origin of the Rotor Axis System, but it is rotated by angles of the swashplate roll and pitch so there is no cyclic feathering in this coordinate system.

Disc Axis System

Origin of the Disc Axis System is coincident with the origin of the Rotor Axis System, but it is rotated by angles of the rotor cone roll and pitch in such a manner that z-axis is perpendicular to the tip path plane so there is no cyclic flapping in this coordinate system.

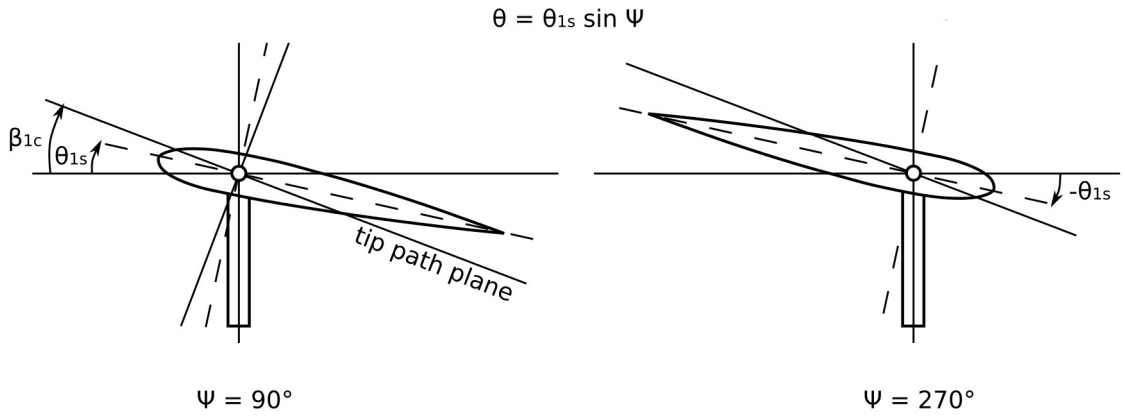

Figure 2-2: Rotor reference planes

Control-Wind Axis System

Control-Wind Axis System is very much like Control Axis System, the only difference is that it is rotated about z-axis in such a manner that x-axis points directly into relative wind, so there is no lateral airspeed component.

Blade Axis System

Blade Axis System is a coordinate system fixed to the rotor blade, its origin is coincident with the intersection point of blade feathering and flapping hinges axes. The x-axis is coincident with blade feathering axis and pointing outwards, the y-axis lies on XY plane of the Control Axis System and points towards blade leading edge, while the z-axis completes a right-handed coordinate system.

Assumptions

Following assumptions are made for the purpose of modeling helicopter rotor aerodynamics:

– forces and moments generated by the rotor are considered to be quasi-steady,

– rotor lift force is a linear function of blade incidence angle and drag force is a quadratic function of lift, [2]

– rotor blades have 3 degrees of freedom movement,

– inflow is uniformly distributed over rotor disc, [2]

– reversed flow effects are ignored,

– airflow is considered to be quasi-steady and incompressible,

– thrust is considered to be parallel to the z-axis of the Control Axis System and magnitude of the thrust is considered to be magnitude of the resulting rotor force. [16]

Momentum Theory

Momentum Theory for Axial Flight

Mass flow through the rotor disc, momentum change and change in kinetic energy are given by the following formulas. [2]

$$\dot{m}=\rho A_1 V_C=\rho A_R\left(V_C+V_I\right)=\rho A_\infty\left(V_C+V_{I\infty}\right) \tag{2.63}$$

$$T=\dot{m}\left(V_C+V_{I\infty}\right)-\dot{m}V_C=\dot{m}V_{I\infty} \tag{2.64}$$

$$T\left(V_C+V_{I\infty}\right)=\frac{1}{2}\dot{m}\left(V_C+V_{I\infty}\right)^2-\frac{1}{2}\dot{m}V_C^2=\frac{1}{2}\dot{m}\left(2V_C V_{I\infty}+V_{I\infty}^2\right) \tag{2.65}$$

where

$A_1=\pi R_1^2$ – [m^2] control volume section area

$A_R=\pi R^2$ – [m^2] rotor disc area

$A_\infty=\pi R_\infty^2$ – [m^2] far wake slipstream section area

$\dot{m}$ – [kg/s] mass flow

V_C – [m/s] climb velocity

V_I – [m/s] induced velocity

$V_{I\infty}$ – [m/s] far wake induced velocity

T – [N] rotor thrust

From these relationships it can be deduced that induced velocity in the far wake is twice the rotor inflow. [2]

$$V_{I\infty}=2V_I \tag{2.66}$$

Substituting equations (2.63) and (2.66) into (2.64) rotor thrust is given as follows.

$$T=2\rho A_R\left(V_C+V_I\right)V_I \tag{2.67}$$

In hover flight, this equation can be expressed as

$$T = 2\rho A_R V_{IH}^2 \tag{2.68}$$

Transforming equations (2.67) and (2.68) gives

$$V_I = \frac{T}{2\rho A_R (V_C + V_I)} \tag{2.69}$$

$$V_{IH} = \sqrt{\frac{T}{2\rho A_R}} \tag{2.70}$$

Writing velocities in normalized form.

$$\lambda_I = \frac{V_I}{\Omega_R R} \tag{2.71}$$

$$\lambda_{IH} = \frac{V_{IH}}{\Omega_R R} \tag{2.72}$$

$$\mu_C = \frac{V_C}{\Omega_R R} \tag{2.73}$$

Rotor thrust coefficient is

$$C_T = \frac{T}{\rho A_R \Omega_R^2 R^2} \tag{2.74}$$

Then equations (2.71) and (2.72) can be expressed as

$$\lambda_I = \frac{C_T}{2(\mu_C + \lambda_I)} \tag{2.75}$$

$$\lambda_{IH} = \sqrt{\frac{C_T}{2}} \tag{2.76}$$

Combining these equations gives

$$\lambda_{IH}^2 = \lambda_I (\mu_C + \lambda_I) \tag{2.77}$$

This equation can be transformed into following form.

$$\lambda_I = -\frac{\mu_C}{2} + \sqrt{\left(\frac{\mu_C}{2}\right)^2 + \lambda_{IH}^2} \tag{2.78}$$

For descent velocity $V_D = -V_C$ formula (2.78) can be written as.

$$\lambda_I = \frac{\mu_D}{2} - \sqrt{\left(\frac{\mu_D}{2}\right)^2 - \lambda_{IH}^2} \tag{2.79}$$

This relationship is valid only in windmill brake state where the wake is fully established and the flow is upwards. [2] It can be assumed that such a condition occurs when descent velocity is two times greater than induced velocity in hover. [17]

Young's approximation can be used to determine induced velocity outside range of momentum theory application. [2]

$$\lambda_I = \lambda_{IH}\left(1+\frac{\mu_D}{\lambda_{IH}}\right) \quad \text{for} \quad 0 \leqslant \mu_D \leqslant -1{,}5\,\lambda_{IH} \tag{2.80}$$

$$\lambda_I = \lambda_{IH}\left(7-3\,\frac{\mu_D}{\lambda_{IH}}\right) \quad \text{for} \quad -1{,}5\,\lambda_{IH} < \mu_D \leqslant -2\,\lambda_{IH} \tag{2.81}$$

Momentum Theory in Forward Flight

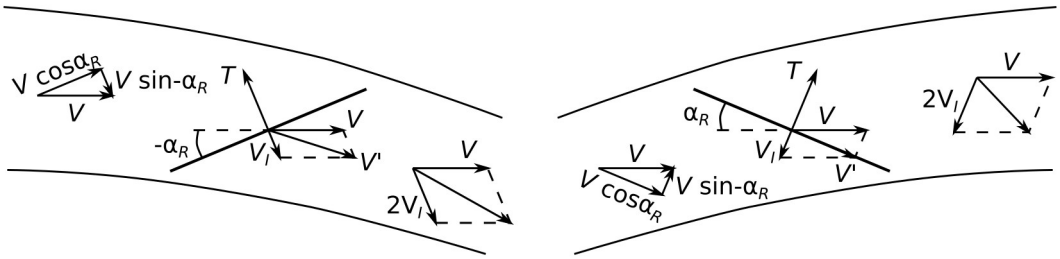

Figure 2-3: Flow trough a rotor in forward flight

In forward flight induced velocity in the far wake is twice the flow at the rotor. [2] Expression for thrust is given as follows.

$$T = \dot{m}\,2V_I = \left(\rho A_R V'\right)2V_I \tag{2.82}$$

Transforming this equation for induced velocity gives.

$$V_I = \frac{T}{2\rho A_R V'} \tag{2.83}$$

where V' is the resultant velocity at the rotor.

$$V' = \sqrt{|\vec{V}|^2 \cos^2\alpha_R + \left(|\vec{V}|\sin\alpha_R - V_I\right)^2} \tag{2.84}$$

Writing velocities in normalized form.

$$\lambda_I = \frac{V_I}{\Omega_R R} \tag{2.85}$$

$$\mu_X = \frac{u_{rw}}{\Omega_R R} \tag{2.86}$$

$$\mu_Z = \frac{w_{rw}}{\Omega_R R} \tag{2.87}$$

where

$$u_{rw} = |\vec{V}| \cos \alpha_R \tag{2.88}$$

$$w_{rw} = |\vec{V}| \sin \alpha_R \tag{2.89}$$

Substituting equations (2.85), (2.86), (2.87) and (2.84) into (2.83) formula for the normalized induced velocity can be expressed as follows.

$$\lambda_I = \frac{C_T}{2\sqrt{\mu_X^2 + (\mu_Z - \lambda_I)^2}} \tag{2.90}$$

In high speed flight summing helicopter translational velocity and velocity due to rotor shaft rotation causes strong non-uniformities of rotor induced velocity. Glauert's model is used to describe this phenomena. [2, 18]

$$\lambda_I(r, \Psi) = \lambda_{I0} + \frac{r}{R} \lambda_{1c} \cos \Psi \tag{2.91}$$

where

$$\lambda_{1c} = \lambda_{I0} \tan\left(\frac{\chi}{2}\right) \quad \text{for} \quad \chi < \frac{\pi}{2} \tag{2.92}$$

$$\lambda_{1c} = \lambda_{I0} \cot\left(\frac{\chi}{2}\right) \quad \text{for} \quad \chi > \frac{\pi}{2} \tag{2.93}$$

The wake angle is given by the following formula

$$\chi = \arctan\left(\frac{\mu}{\lambda_{I0} - \mu_Z}\right) \tag{2.94}$$

where λ_{I0} is given by formula (2.90).

Blade Element Theory

Determining forces and moments acting on segment of the blade is made using blade element theory, assuming that blade is composed of aerodynamically independent, narrow strips of elements. [17] High aspect ratio of the blade justifies usage of two-dimensional flow, while lift loss at the blade tip and root can be accounted by using tip-loss factor. [2, 17, 18]

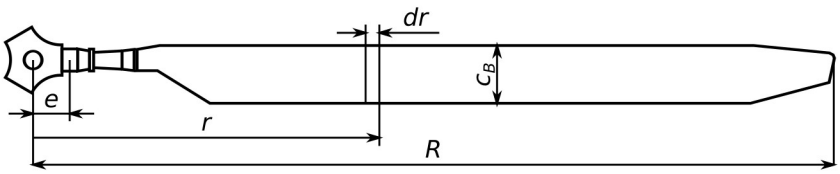

Figure 2-4: Rotor blade element

Control-Wind Axis System is used to determine forces and moments generated by the rotor, such computed forces and moments are the transformed to the Body Axis System.

Lift and drag acting on a blade section is given by the following expressions.

$$dL = \frac{1}{2}\rho U^2(r,\Psi) C_L c_B dr \tag{2.95}$$

$$dD = \frac{1}{2}\rho U^2(r,\Psi) C_D c_B dr \tag{2.96}$$

Lift and drag coefficients are given as follows. [2]

$$C_L = a\,\alpha_{BE}(r,\Psi) \tag{2.97}$$

$$C_D = \delta_0 + \delta_2 C_T^2 \tag{2.98}$$

Blade section angle of attack is given by the following formula.

$$\alpha_{BE}(r,\Psi) = \theta + \phi(r,\Psi) \tag{2.99}$$

where

$$\phi(r,\Psi) = \arctan\frac{U_P(r,\Psi)}{U_T(r,\Psi)} \tag{2.100}$$

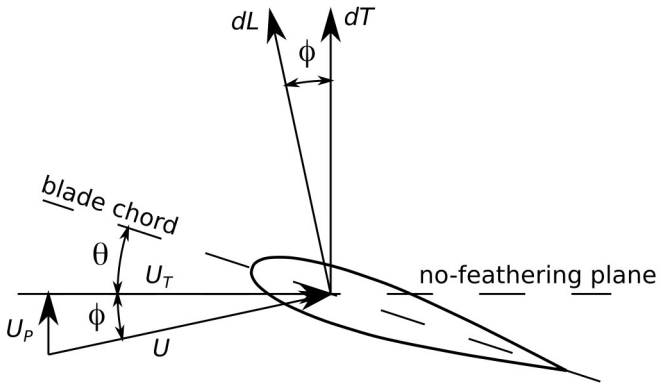

Figure 2-5: Velocity components at the blade element

Air Velocity at the Blade Element

Linear velocity of the rotor hub and angular velocity expressed Rotor Axis System are given by the following formulas. [17, 18]

$$\vec{V}_{RH,r} = \boldsymbol{T}(\varepsilon)\left(\vec{V}_{O,b} + \vec{\omega}_b \times \vec{r}_{RH,b}\right) \tag{2.101}$$

$$\vec{\Omega}_r = \boldsymbol{T}(\varepsilon)\vec{\Omega}_b \tag{2.102}$$

where

$$\boldsymbol{T}(\varepsilon)=\begin{bmatrix}\cos\varepsilon & 0 & \sin\varepsilon\\ 0 & 1 & 0\\ -\sin\varepsilon & 0 & \cos\varepsilon\end{bmatrix} \tag{2.103}$$

Following formulas can be used to transform this values to Control Axis System.

$$\vec{V}_{RH,c}=\boldsymbol{T}\left(\theta_{1c},\theta_{1s}\right)\vec{V}_{RH,r} \tag{2.104}$$
$$\vec{\Omega}_{c}=\boldsymbol{T}\left(\theta_{1c},\theta_{1s}\right)\vec{\Omega}_{r}$$

where rotation matrix is:

– for counterclockwise direction of rotor

$$\boldsymbol{T}\left(\theta_{1c},\theta_{1s}\right)=\begin{bmatrix}1 & 0 & 0\\ 0 & \cos\theta_{1c} & -\sin\theta_{1c}\\ 0 & \sin\theta_{1c} & \cos\theta_{1c}\end{bmatrix}\begin{bmatrix}\cos\theta_{1s} & 0 & -\sin\theta_{1s}\\ 0 & 1 & 0\\ \sin\theta_{1s} & 0 & \cos\theta_{1s}\end{bmatrix} \tag{2.105}$$

– for clockwise direction of rotor

$$\boldsymbol{T}\left(\theta_{1c},\theta_{1s}\right)=\begin{bmatrix}1 & 0 & 0\\ 0 & \cos\theta_{1c} & \sin\theta_{1c}\\ 0 & -\sin\theta_{1c} & \cos\theta_{1c}\end{bmatrix}\begin{bmatrix}\cos\theta_{1s} & 0 & -\sin\theta_{1s}\\ 0 & 1 & 0\\ \sin\theta_{1s} & 0 & \cos\theta_{1s}\end{bmatrix} \tag{2.106}$$

Following formulas can be used to transform linear and angular velocity vector to Control-Wind Axis System.

$$\vec{V}_{RH,cw}=\boldsymbol{T}(\beta)\vec{V}_{RH,c} \tag{2.107}$$
$$\vec{\Omega}_{cw}=\boldsymbol{T}(\beta)\vec{\Omega}_{c} \tag{2.108}$$

Where $\boldsymbol{T}(\beta)$ is given by formula (2.46).

Assuming that flapping angle is positive upwards and writing velocity components as

$$\vec{V}_{RH,cw}=\left[u_{cw},0,w_{cw}\right]^{T} \tag{2.109}$$
$$\vec{\Omega}_{cw}=\left[p_{cw},q_{cw},0\right]^{T} \tag{2.110}$$

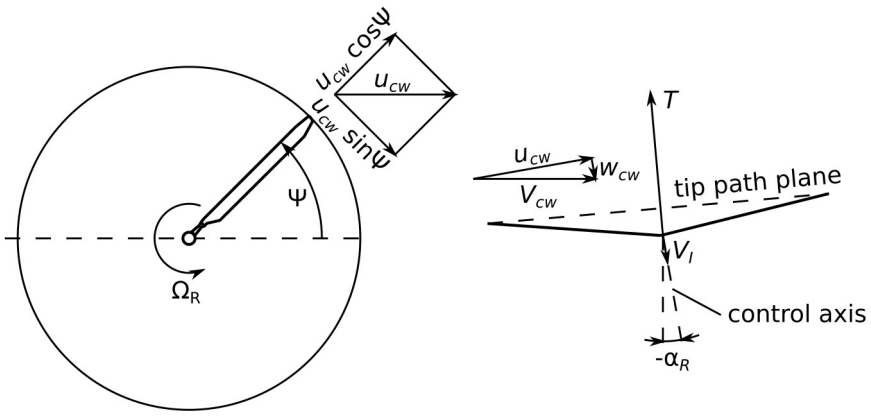

Figure 2-6: Air velocities at the blade element

Air velocity at the blade element is:

– for counterclockwise direction of rotor

$$U_T = \Omega_R r \cos\beta + u_{cw} \sin\Psi \tag{2.111}$$

$$U_P = w_{cw}\cos\beta - v_i \cos\beta - \dot{\beta} r - u_{cw} \sin\beta \cos\Psi + p_{cw} r \sin\Psi + q_{cw} r \cos\Psi \tag{2.112}$$

– for clockwise direction of rotor

$$U_T = \Omega_R r \cos\beta + u_{cw} \sin\Psi \tag{2.113}$$

$$U_P = w_{cw}\cos\beta - V_I \cos\beta - \dot{\beta} r - u_{cw} \sin\beta \cos\Psi - p_{cw} r \sin\Psi + q_{cw} r \cos\Psi \tag{2.114}$$

Assuming that for small angles:

$$\sin\beta \approx \beta \tag{2.115}$$

$$\cos\beta \approx 1 \tag{2.116}$$

This expressions can be simplified to:

– for counterclockwise direction of rotor

$$U_T = \Omega_R r + u_{cw} \sin\Psi \tag{2.117}$$

$$U_P = w_{cw} - V_I - \dot{\beta} r - u_{cw}\beta \cos\Psi + p_{cw} r \sin\Psi + q_{cw} r \cos\Psi \tag{2.118}$$

– for clockwise direction of rotor

$$U_T = \Omega_R r + u_{cw} \sin\Psi \tag{2.119}$$

$$U_P = w_{cw} - V_I - \dot{\beta} r - u_{cw}\beta \cos\Psi - p_{cw} r \sin\Psi + q_{cw} r \cos\Psi \tag{2.120}$$

Using normalized velocities

$$\mu = \frac{u_{cw}}{\Omega_R R} \tag{2.121}$$

$$\lambda = \frac{w_{cw} - V_I}{\Omega_R R} \tag{2.122}$$

Expressions for air velocity at the blade element can be written in the following form:

– for counterclockwise direction of rotor

$$U_T = \Omega_R r + \mu \Omega_R R \sin \Psi \tag{2.123}$$

$$U_P = \lambda \Omega_R R - \dot{\beta} r - \mu \Omega_R R \beta \cos \Psi + p_{cw} r \sin \Psi + q_{cw} r \cos \Psi \tag{2.124}$$

– for clockwise direction of rotor

$$U_T = \Omega_R r + \mu \Omega_R R \sin \Psi \tag{2.125}$$

$$U_P = \lambda \Omega_R R - \dot{\beta} r - \mu \Omega_R R \beta \cos \Psi - p_{cw} r \sin \Psi + q_{cw} r \cos \Psi \tag{2.126}$$

Rotor Thrust

Assuming that for small angles.

$$\phi = \arctan \frac{U_P}{U_T} \approx \frac{U_P}{U_T} \tag{2.127}$$

$$U \approx U_T \tag{2.128}$$

$$dT \approx dL \tag{2.129}$$

Expression for the blade element angle of attack is given as follows.

$$\alpha_{BE} = \theta + \frac{U_P}{U_T} \tag{2.130}$$

Then expression (2.97) can be written as. [16]

$$C_L = a\left(\theta + \frac{U_P}{U_T}\right) \tag{2.131}$$

Substituting expression (2.95) and taking into account simplifications (2.127), (2.128) and (2.129) then rotor thrust is given by the following formula.

$$dT \approx \frac{1}{2} \rho a c_B U_T^2 \left(\theta + \frac{U_P}{U_T}\right) dr \tag{2.132}$$

Transforming this relationship gives.

$$dT \approx \frac{1}{2} \rho a c_B \left(\theta U_T^2 + U_P U_T\right) dr \tag{2.133}$$

Total thrust generated by the rotor of N_B blades can be determined by integrating differential equation (2.133) first with respect to the azimuth then along the blade span. [16] Total thrust is given as follows.

$$T=\frac{N_b}{2\pi}\int_0^{2\pi}\int_0^{BR}\frac{dT}{dr}dr\,d\Psi \tag{2.134}$$

Where B is a tip loss factor.

Substituting (2.133) into (2.134) gives.

$$T=\frac{1}{2}\rho a c_B N_b\left(\theta\frac{1}{2\pi}\int_0^{2\pi}\int_0^{BR}\frac{U_T^2}{dr}dr\,d\Psi+\frac{1}{2\pi}\int_0^{2\pi}\int_0^{BR}U_P U_T\,dr\,dr\,d\Psi\right) \tag{2.135}$$

Neglecting helicopter angular velocity expressions for U_T^2 and $U_P U_T$ can be written as.

$$U_T^2=r^2\Omega_R^2+2\Omega_R^2 R\,r\,\mu\sin\Psi+\mu^2R^2\Omega_R^2\sin^2\Psi \tag{2.136}$$

$$\begin{gathered}U_P U_T=\lambda\Omega_R^2 R r-\dot{\beta}\Omega_R r^2-\beta\mu\Omega_R^2 R\,r\cos\Psi\\+\lambda\mu\Omega_R^2R^2\sin\Psi-\dot{\beta}\mu\Omega_R R r\sin\Psi-\beta\mu^2\Omega_R^2R^2\sin\Psi\cos\Psi\end{gathered} \tag{2.137}$$

Expression for the blade flapping angle can be written as follows. [2, 16, 19]

$$\beta(\Psi)=\beta_0+\beta_{1c}\cos\Psi+\beta_{1s}\sin\Psi \tag{2.138}$$

Assuming constant rotor revolution speed, blade flapping angle derivatives with respect to time can be written as derivatives with respect to the azimuth. [16]

$$\dot{\beta}=\frac{d\beta}{dt}=\frac{d\beta}{d\Psi}\frac{d\Psi}{dt}=\bar{\beta}\Omega_R=\Omega_R\left(\beta_{1s}\cos\Psi-\beta_{1c}\sin\Psi\right) \tag{2.139}$$

$$\ddot{\beta}=\frac{d^2\beta}{dt^2}=\frac{d^2\beta}{d\Psi^2}\left(\frac{d\Psi}{dt}\right)^2=\bar{\bar{\beta}}\Omega_R^2=-\Omega_R^2\left(\beta_{1c}\cos\Psi+\beta_{1s}\sin\Psi\right) \tag{2.140}$$

Then expressions for U_T^2 and $U_P U_T$ can be written as.

$$U_T^2=r^2\Omega_R^2+2\Omega_R^2 R\,r\,\mu\sin\Psi+\mu^2R^2\Omega_R^2\sin^2\Psi \tag{2.141}$$

$$\begin{gathered}U_P U_T=\lambda\Omega_R^2 R r-\beta_{1s}\Omega_R^2 r^2\cos\Psi+\beta_{1c}\Omega_R^2 r^2\sin\Psi-\beta\mu\Omega_R^2 R\,r\cos\Psi\\+\lambda\mu\Omega_R^2R^2\sin\Psi-\beta_{1s}\mu\Omega_R^2 R r\sin\Psi\cos\Psi+\beta_{1c}\mu\Omega_R^2 R\,r\sin^2\Psi-\beta\mu^2\Omega_R^2R^2\sin\Psi\cos\Psi\end{gathered} \tag{2.142}$$

Knowing that [16]

$$\frac{1}{2\pi}\int_0^{2\pi}\sin\Psi\,d\Psi=0 \tag{2.143}$$

$$\frac{1}{2\pi}\int_0^{2\pi}\sin^2\Psi\,d\Psi=\frac{1}{2} \tag{2.144}$$

$$\frac{1}{2\pi}\int_0^{2\pi}\sin\Psi\cos\Psi\,d\Psi=0 \tag{2.145}$$

$$\frac{1}{2\pi}\int_0^{2\pi}\cos\Psi\,d\Psi=0 \tag{2.146}$$

$$\frac{1}{2\pi}\int_0^{2\pi}\cos^2\Psi\,d\Psi=\frac{1}{2} \tag{2.147}$$

Rotor thrust can be written as.

$$T=\frac{1}{2}\rho a c_B N_b \Omega_R^2 R^3 B\left[\frac{\lambda B}{2}+\frac{\theta}{3}\left(B^2+\frac{3}{2}\mu^2\right)+\frac{\beta_{1c}B}{4}\mu\right] \tag{2.148}$$

Using expression (2.74) rotor thrust coefficient is given by the following formula.

$$C_T=\frac{1}{2}a s B\left[\frac{\lambda B}{2}+\frac{\theta}{3}\left(B^2+\frac{3}{2}\mu^2\right)+\frac{\beta_{1c}B}{4}\mu\right] \tag{2.149}$$

Where *s* is rotor solidity.

Rotor Torque

The torque on a blade element is given by the following formula. [16, 18]

$$dQ=r\left(dD\cos\phi-dL\sin\phi\right)dr \tag{2.150}$$

Assuming that for small angles

$$\sin\phi\approx\phi \tag{2.151}$$

$$\cos\phi\approx 1 \tag{2.152}$$

and assuming that drag coefficient is constant along blade span, expression (2.150) can be written as. [16, 18]

$$dQ=\frac{1}{2}\rho U_T^2 C_D c_B r\,dr-\frac{1}{2}\rho U_T^2 C_L c_B r\,\phi dr \tag{2.153}$$

Torque due to the profile drag can be expressed as [18].

$$Q_p=\frac{N_b}{2\pi}\int_0^R\int_0^{2\pi}\frac{1}{2}\rho U_T^2 C_D c_B r\,d\Psi\,dr \tag{2.154}$$

Substituting (2.136) and integrating this equation first with respect to the azimuth then along the blade span gives.

$$Q_p=\frac{1}{2}\rho N_b c_B \Omega_R^2 R^4 C_D\left(\frac{1}{4}+\frac{1}{4}\mu^2\right) \tag{2.155}$$

Induced torque is given by the following formula. [18]

$$Q_I=\frac{N_b}{2\pi}\int_0^R\int_0^{2\pi}\frac{1}{2}\rho U_T^2 C_L c_B r\,\phi d\Psi\,dr \tag{2.156}$$

Substituting (2.127) and (2.131) gives.

$$Q_I=\frac{N_b}{2\pi}\frac{1}{2}\rho a c_B\int_0^R\int_0^{2\pi}\left(\theta U_P U_T r+U_P^2 r\right)d\Psi\,dr \tag{2.157}$$

Neglecting helicopter angular velocity expressions for U_P^2 can be written as.

$$\begin{aligned} U_P^2 = \dot{\beta}^2 r^2 + 2\beta\dot{\beta}\mu\Omega_R R r\cos\Psi - 2\dot{\beta}\lambda\Omega_R R r \\ + \beta^2\mu^2\Omega_R^2 R^2(\cos\Psi)^2 - 2\beta\lambda\mu\Omega_R^2 R^2\cos\Psi + \lambda^2\Omega_R^2 R^2 \end{aligned} \tag{2.158}$$

Substituting (2.137) and (2.158) into (2.157) and integrating equation (2.157) first with respect to the azimuth then along the blade span gives.

$$Q_I = \frac{1}{2}\rho a c_B N_b \Omega_R^2 R^4 \left[\begin{array}{c} \frac{1}{3}\lambda\theta + \frac{1}{2}\lambda^2 - \frac{1}{8}\left(\beta_{1c}^2 + \beta_{1s}^2\right) \\ + \frac{1}{2}\mu^2\left(\frac{\beta_0^2}{2} - \frac{3}{8}\beta_{1c}^2 - \frac{1}{8}\beta_{1s}^2\right) - \frac{1}{2}\mu\lambda\beta_{1c} + \frac{1}{3}\mu\beta_0\beta_{1s} \end{array} \right] \tag{2.159}$$

The total rotor torque is given as follows.

$$Q = Q_P + Q_I \tag{2.160}$$

$$Q = \frac{1}{2}\rho a c_B N_b \omega_R^2 R^4 \left[\begin{array}{c} \frac{C_D}{4a}\left(1+\mu^2\right) - \frac{1}{3}\lambda\theta - \frac{1}{2}\lambda^2 + \frac{1}{8}\left(\beta_{1c}^2 + \beta_{1s}^2\right) \\ - \frac{1}{2}\mu^2\left(\frac{\beta_0^2}{2} - \frac{3}{8}\beta_{1c}^2 - \frac{1}{8}\beta_{1s}^2\right) + \frac{1}{2}\mu\lambda\beta_{1c} - \frac{1}{3}\mu\beta_0\beta_{1s} \end{array} \right] \tag{2.161}$$

Rotor torque coefficient can be written as.

$$C_Q = \frac{1}{2}as \left[\begin{array}{c} \frac{C_D}{4a}\left(1+\mu^2\right) - \frac{1}{3}\lambda\theta - \frac{1}{2}\lambda^2 + \frac{1}{8}\left(\beta_{1c}^2 + \beta_{1s}^2\right) \\ - \frac{1}{2}\mu^2\left(\frac{\beta_0^2}{2} - \frac{3}{8}\beta_{1c}^2 - \frac{1}{8}\beta_{1s}^2\right) + \frac{1}{2}\mu\lambda\beta_{1c} - \frac{1}{3}\mu\beta_0\beta_{1s} \end{array} \right] \tag{2.162}$$

Flapping Coefficients

Expressions for blades flapping coefficients can be derived from the equation of moments equilibrium about flapping hinge using method described in [19].

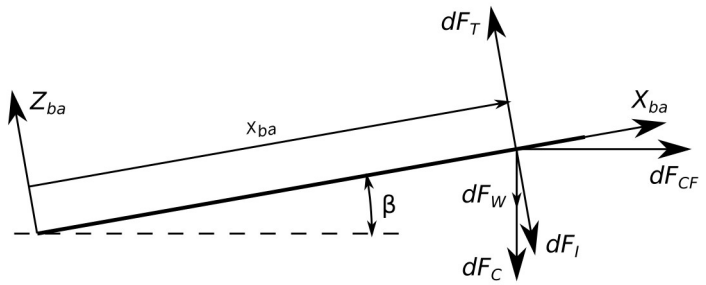

Figure 2-7: Forces acting on the blade element

Moments equilibrium about flapping hinge can be written as follows. [16]

$$M_I + M_{CF} + M_C + M_T + M_W = 0 \tag{2.163}$$

where

M_I – [N] moment of inertia forces of flapping

M_{CF} – [N] moment of centrifugal force

M_C – [N] moment of Coriolis force

M_T – [N] moment of thrust

M_W – [N] moment of weight

Moments of Inertia Forces

Assuming that rotor revolution speed is constant, helicopter angular velocities are constant and rotor blades are able to move about flapping hinge axis while neglecting helicopter yaw motion and blades pitching and lagging motion then centrifugal force can be written as.

$$dF_{CF} = m_B \Omega_R^2 r \, dr \tag{2.164}$$

Component of the Coriolis force laying on the flapping plane is given:

– for counterclockwise direction of rotor

$$dF_C = 2 m_B p_{cw} \Omega_R r \cos\Psi \, dr - 2 m_B q_{cw} \Omega_R r \sin\Psi \, dr \tag{2.165}$$

– for clockwise direction of rotor

$$dF_C = -2 m_B p_{cw} \Omega_R r \cos\Psi \, dr - 2 m_B q_{cw} \Omega_R r \sin\Psi \, dr \tag{2.166}$$

Moment of inertia forces of flapping is given by the following formula.

$$M_I = -\ddot{\beta} \int_0^R m_B r^2 \, dr \tag{2.167}$$

Assuming that rotor blades are homogeneous rods blade first moment of mass and moment of inertia can be written as. [19]

$$J_B \approx \int_0^R m_B r^2 \, dr \tag{2.168}$$

$$S_B \approx \int_0^R m_B r \, dr \tag{2.169}$$

Hence

$$M_I = -\ddot{\beta} J_B \tag{2.170}$$

Taking into account (2.115) and (2.116) moment of centrifugal forces if.

$$M_{CF} = -\int_0^R \beta m_B \Omega_R^2 r^2 dr = -\Omega_R^2 \beta \int_0^R m_B r^2 dr \tag{2.171}$$

Substituting (2.168) into (2.171) gives.

$$M_{CF} = -\Omega_R^2 \beta J_B \tag{2.172}$$

Moment of Coriolis forces can be writes as:

– for counterclockwise direction of rotor

$$\begin{gathered} M_C = 2\int_0^R m_B p_{cw} \Omega_R r^2 \cos\Psi \, dr - 2\int_0^R m_B q_{cw} \Omega_R r^2 \sin\Psi \, dr = \\ = 2 p_{cw} \Omega_R J_B \cos\Psi - 2 q_{cw} \Omega_R J_B \sin\Psi \end{gathered} \tag{2.173}$$

– for clockwise direction of rotor

$$\begin{gathered} M_C = -2\int_0^R m_B p_{cw} \Omega_R r^2 \cos\Psi \, dr - 2\int_0^R m_B q_{cw} \Omega_R r^2 \sin\Psi \, dr = \\ = -2 p_{cw} \Omega_R J_B \cos\Psi - 2 q_{cw} \Omega_R J_B \sin\Psi \end{gathered} \tag{2.174}$$

Using approximation (2.169) moment due to weight can expressed as.

$$M_W = -g\int_0^R m_B r \, dr = -g S_B \tag{2.175}$$

Moment of Thrust

Using equation (2.133) expression for moment of thrust about flapping hinge can be written as follows.

$$M_T = \int_0^{BR} dT \, r = \frac{1}{2} \rho a c_B \int_0^{BR} \left(\theta U_T^2 + U_P U_T \right) dr \tag{2.176}$$

Equilibrium of Moments about Flapping Hinge

Substituting into (2.163) expressions for moments of thrust, weight, inertia, centrifugal and Coriolis forces moments equilibrium equation is given as:

– for counterclockwise direction of rotor

$$\int_0^{BR} dT \, r - \ddot{\beta} J_B - \beta \Omega_R^2 J_B + 2 p_{cw} \Omega_R J_B \cos\Psi - 2 q_{cw} \Omega_R J_B \sin\Psi - g S_B = 0 \tag{2.177}$$

$$-J_B \ddot{\beta} - J_B \beta \Omega_R^2 + \int_0^{BR} dT \, r = 2 J_B q_{cw} \Omega_R \sin\Psi - 2 J_B p_{cw} \Omega_R \cos\Psi + g S_B \tag{2.178}$$

– for clockwise direction of rotor

$$\int_0^{BR} dT\, r - \ddot{\beta} J_B - \beta \Omega_R^2 J_B - 2\, p_{cw} \Omega_R J_B \cos\Psi - 2\, q_{cw} \Omega_R J_B \sin\Psi - g\, S_B = 0 \tag{2.179}$$

$$-J_B \ddot{\beta} - J_B \beta \Omega_R^2 + \int_0^{BR} dT\, r = 2\, J_B q_{cw} \Omega_R \sin\Psi + 2\, J_B p_{cw} \Omega_R \cos\Psi + g\, S_B \tag{2.180}$$

Dividing both sides of equations (2.178) and (2.180) by $J_B \Omega_R^2$ gives.

$$\ddot{\beta} + \beta = \frac{1}{J_B \Omega_R^2} \int_0^{BR} dT\, r - 2\frac{q_{cw}}{\Omega_R} \sin\Psi + 2\frac{p_{cw}}{\Omega_R} \cos\Psi - \frac{g\, S_B}{J_B \Omega_R^2} \tag{2.181}$$

$$\ddot{\beta} + \beta = \frac{1}{J_B \Omega_R^2} \int_0^{BR} dT\, r - 2\frac{q_{cw}}{\Omega_R} \sin\Psi - 2\frac{p_{cw}}{\Omega_R} \cos\Psi - \frac{g\, S_B}{J_B \Omega_R^2} \tag{2.182}$$

Substituting expressions (2.136) and (2.137) into (2.181) and (2.182) gives.

$$M_T = \int_0^{BR} dT\, r = \frac{1}{2} \rho a\, c_B \int_0^{BR} \left(\theta U_T^2 + U_P U_T \right) r\, dr =$$

$$= \frac{1}{2} \rho a\, c_B R^4 \Omega_R^2 \left(\begin{array}{c} \frac{B^4}{4}\theta + \frac{2}{3} B^3 \theta\mu \sin\Psi + \frac{B^2}{2} \theta\mu^2 \sin^2\Psi \\ + \frac{B^3}{3}\lambda - \frac{B^4}{4}\bar{\beta} - \frac{B^3}{3}\beta\mu \cos\Psi + \frac{B^4}{4}\frac{p_{cw}}{\Omega_R} \sin\Psi \\ + \frac{B^2}{2}\lambda\mu \sin\Psi - \frac{B^2}{2}\beta\mu^2 \sin\Psi \cos\Psi - \frac{B^3}{3}\bar{\beta}\mu \sin\Psi \\ + \frac{B^3}{3}\frac{p_{cw}}{\Omega_R}\mu \sin^2\Psi + \frac{B^4}{4}\frac{q_{cw}}{\Omega_R}\cos\Psi + \frac{B^3}{3}\frac{q_{cw}}{\Omega_R}\mu \sin\Psi \cos\Psi \end{array} \right) \tag{2.183}$$

$$M_T = \int_0^{BR} dT\, r = \frac{1}{2} \rho a\, c_B \int_0^{BR} \left(\theta U_T^2 + U_P U_T \right) dr =$$

$$= \frac{1}{2} \rho a\, c_B R^4 \Omega_R^2 \left(\begin{array}{c} \frac{B^4}{4}\theta + \frac{2}{3} B^3 \theta\mu \sin\Psi + \frac{B^2}{2} \theta\mu^2 \sin^2\Psi \\ + \frac{B^3}{3}\lambda - \frac{B^4}{4}\bar{\beta} - \frac{B^3}{3}\beta\mu \cos\Psi - \frac{B^4}{4}\frac{p_{cw}}{\Omega_R} \sin\Psi \\ + \frac{B^2}{2}\lambda\mu \sin\Psi - \frac{B^2}{2}\beta\mu^2 \sin\Psi \cos\Psi - \frac{B^3}{3}\bar{\beta}\mu \sin\Psi \\ - \frac{B^3}{3}\frac{p_{cw}}{\Omega_R}\mu \sin^2\Psi + \frac{B^4}{4}\frac{q_{cw}}{\Omega_R}\cos\Psi + \frac{B^3}{3}\frac{q_{cw}}{\Omega_R}\mu \sin\Psi \cos\Psi \end{array} \right) \tag{2.184}$$

Knowing that

$$\sin\Psi\cos\Psi=\frac{\sin(2\Psi)}{2} \qquad \sin^2\Psi=\frac{1-\cos(2\Psi)}{2} \qquad \cos\Psi\sin(2\Psi)=\frac{\sin\Psi+\sin(3\Psi)}{2} \tag{2.185}$$

$$\cos^2\Psi=\frac{1+\cos(2\Psi)}{2} \qquad \sin\Psi\sin(2\Psi)=\frac{\cos\Psi-\cos(3\Psi)}{2} \tag{2.186}$$

(2.187)

(2.188)

(2.189)

Substituting (2.183) into (2.181) and (2.184) into (2.182) gives.

$$\begin{aligned}
&\bar{\bar{\beta}}+\bar{\beta}\frac{\gamma}{2}\left(\frac{B^4}{4}+\frac{B^3}{3}\mu\sin\Psi\right)+\beta\left(1+\frac{B^3}{6}\gamma\mu\cos\Psi+\frac{B^2}{8}\gamma\mu^2\sin(2\Psi)\right)=\\
&=\frac{\gamma}{2}\left(\begin{array}{c}\frac{B^3}{3}\lambda+\frac{B^4}{4}\frac{p_{cw}}{\Omega_R}\sin\Psi+\frac{B^2}{2}\lambda\mu\sin\Psi+\frac{B^3}{6}\frac{p_{cw}}{\Omega_R}\mu-\frac{B^3}{6}\frac{p_{cw}}{\Omega_R}\mu\cos(2\Psi)\\ +\frac{B^4}{4}\frac{q_{cw}}{\Omega_R}\cos\Psi+\frac{B^3}{6}\frac{q_{cw}}{\Omega_R}\mu\sin(2\Psi)+\frac{B^4}{4}\theta\\ +\frac{2}{3}B^3\theta\mu\sin\Psi+\frac{B^2}{4}\theta\mu^2-\frac{B^2}{4}\theta\mu^2\cos(2\Psi)\end{array}\right)\\
&\qquad -2\frac{q_{cw}}{\Omega_R}\sin\Psi+2\frac{p_{cw}}{\Omega_R}\cos\Psi-\frac{gS_B}{J_B\Omega_R^2}
\end{aligned} \tag{2.190}$$

$$\begin{aligned}
&\bar{\bar{\beta}}+\bar{\beta}\frac{\gamma}{2}\left(\frac{B^4}{4}+\frac{B^3}{3}\mu\sin\Psi\right)+\beta\left(1+\frac{B^3}{6}\gamma\mu\cos\Psi+\frac{B^2}{8}\gamma\mu^2\sin(2\Psi)\right)=\\
&=\frac{\gamma}{2}\left(\begin{array}{c}\frac{B^3}{3}\lambda-\frac{B^4}{4}\frac{p_{cw}}{\Omega_R}\sin\Psi+\frac{B^2}{2}\lambda\mu\sin\Psi-\frac{B^3}{6}\frac{p_{cw}}{\Omega_R}\mu+\frac{B^3}{6}\frac{p_{cw}}{\Omega_R}\mu\cos(2\Psi)\\ +\frac{B^4}{4}\frac{q_{cw}}{\Omega_R}\cos\Psi+\frac{B^3}{6}\frac{q_{cw}}{\Omega_R}\mu\sin(2\Psi)+\frac{B^4}{4}\theta\\ +\frac{2}{3}B^3\theta\mu\sin\Psi+\frac{B^2}{4}\theta\mu^2-\frac{B^2}{4}\theta\mu^2\cos(2\Psi)\end{array}\right)\\
&\qquad -2\frac{q_{cw}}{\Omega_R}\sin\Psi-2\frac{p_{cw}}{\Omega_R}\cos\Psi-\frac{gS_B}{J_B\Omega_R^2}
\end{aligned} \tag{2.191}$$

where γ is a blade Lock number.

Transforming equations (2.190) and (2.191) gives.

$$\begin{aligned}
&\ddot{\bar{\beta}}+\bar{\beta}\frac{\gamma}{2}\left(\frac{B^4}{4}+\frac{B^3}{3}\mu\sin\Psi\right)+\beta\left(1+\frac{B^3}{6}\gamma\mu\cos\Psi+\frac{B^2}{8}\gamma\mu^2\sin(2\Psi)\right)= \\
&=\left[\frac{\gamma}{2}\left(\frac{B^3}{3}\lambda+\frac{B^3}{6}\frac{p_{cw}}{\Omega_R}\mu+\frac{B^4}{4}\theta+\frac{B^2}{4}\theta\mu^2\right)-\frac{gS_B}{J_B\Omega_R^2}\right] \\
&+\left[\frac{\gamma}{2}\left(\frac{B^4}{4}\frac{q_{cw}}{\Omega_R}\right)+2\frac{p_{cw}}{\Omega_R}\right]\cos\Psi \\
&+\left[\frac{\gamma}{2}\left(\frac{B^4}{4}\frac{p_{cw}}{\Omega_R}+\frac{B^2}{2}\lambda\mu+\frac{2}{3}B^3\theta\mu\right)-2\frac{q_{cw}}{\Omega_R}\right]\sin\Psi \\
&+\left[\frac{\gamma}{2}\left(-\frac{B^3}{6}\frac{p_{cw}}{\Omega_R}\mu-\frac{B^2}{4}\theta\mu^2\right)\right]\cos(2\Psi) \\
&+\left[\frac{\gamma}{2}\left(\frac{B^3}{6}\frac{q_{cw}}{\Omega_R}\mu\right)\right]\sin(2\Psi)
\end{aligned} \tag{2.192}$$

$$\begin{aligned}
&\ddot{\bar{\beta}}+\bar{\beta}\frac{\gamma}{2}\left(\frac{B^4}{4}+\frac{B^3}{3}\mu\sin\Psi\right)+\beta\left(1+\frac{B^3}{6}\gamma\mu\cos\Psi+\frac{B^2}{8}\gamma\mu^2\sin(2\Psi)\right)= \\
&=\left[\frac{\gamma}{2}\left(\frac{B^3}{3}\lambda-\frac{B^3}{6}\frac{p_{cw}}{\Omega_R}\mu+\frac{B^4}{4}\theta+\frac{B^2}{4}\theta\mu^2\right)-\frac{gS_B}{J_B\Omega_R^2}\right] \\
&+\left[\frac{\gamma}{2}\left(\frac{B^4}{4}\frac{q_{cw}}{\Omega_R}\right)-2\frac{p_{cw}}{\Omega_R}\right]\cos\Psi \\
&+\left[\frac{\gamma}{2}\left(-\frac{B^4}{4}\frac{p_{cw}}{\Omega_R}+\frac{B^2}{2}\lambda\mu+\frac{2}{3}B^3\theta\mu\right)-2\frac{q_{cw}}{\Omega_R}\right]\sin\Psi \\
&+\left[\frac{\gamma}{2}\left(\frac{B^3}{6}\frac{p_{cw}}{\Omega_R}\mu-\frac{B^2}{4}\theta\mu^2\right)\right]\cos(2\Psi) \\
&+\left[\frac{\gamma}{2}\left(\frac{B^3}{6}\frac{q_{cw}}{\Omega_R}\mu\right)\right]\sin(2\Psi)
\end{aligned} \tag{2.193}$$

Differentiating equation (2.138) gives.

$$\dot{\bar{\beta}}=\left(\beta_{1s}\cos\Psi-\beta_{1c}\sin\Psi\right) \tag{2.194}$$

$$\ddot{\bar{\beta}}=-\left(\beta_{1c}\cos\Psi+\beta_{1s}\sin\Psi\right) \tag{2.195}$$

Substituting expressions (2.194) and (2.195) into equations (2.192) and (2.193) as well as using trigonometric identities (2.185), (2.186), (2.187), (2.188) and (2.189) gives.

$$\begin{aligned}
&\beta_0+\beta_{1s}\gamma\frac{B^2}{8}\left(\frac{\mu^2}{2}+B^2\right)\cos\Psi+\beta_{1c}\gamma\frac{B^2}{8}\left(\frac{\mu^2}{2}-B^2\right)\sin\Psi\\
&+\beta_{1c}\gamma\frac{B^3}{6}\mu\cos(2\Psi)+\left(\beta_{1s}\gamma\frac{B^3}{6}\mu+\beta_0\gamma\frac{B^2}{8}\mu^2\right)\sin(2\Psi)\\
&+\beta_{1c}\gamma\frac{B^2}{16}\mu^2\sin(3\Psi)-\beta_{1s}\gamma\frac{B^2}{16}\mu^2\cos(3\Psi)=\\
&=\left[\frac{\gamma}{2}\left(\frac{B^3}{3}\lambda+\frac{B^3}{6}\frac{p_{cw}}{\Omega_R}\mu+\frac{B^4}{4}\theta+\frac{B^2}{4}\theta\mu^2\right)-\frac{gS_B}{J_B\Omega_R^2}\right]\\
&+\left[\frac{\gamma}{2}\left(\frac{B^4}{4}\frac{q_{cw}}{\Omega_R}-\frac{B^3}{3}\beta_0\mu\right)+2\frac{p_{cw}}{\Omega_R}\right]\cos\Psi\\
&+\left[\frac{\gamma}{2}\left(\frac{B^4}{4}\frac{p_{cw}}{\Omega_R}+\frac{B^2}{2}\lambda\mu+\frac{2}{3}B^3\theta\mu\right)-2\frac{q_{cw}}{\Omega_R}\right]\sin\Psi\\
&+\left[\frac{\gamma}{2}\left(-\frac{B^3}{6}\frac{p_{cw}}{\Omega_R}\mu-\frac{B^2}{4}\theta\mu^2\right)\right]\cos(2\Psi)\\
&+\left[\frac{\gamma}{2}\left(\frac{B^3}{6}\frac{q_{cw}}{\Omega_R}\mu\right)\right]\sin(2\Psi)
\end{aligned}\tag{2.196}$$

$$\begin{aligned}
&\beta_0+\beta_{1s}\gamma\frac{B^2}{8}\left(\frac{\mu^2}{2}+B^2\right)\cos\Psi+\beta_{1c}\gamma\frac{B^2}{8}\left(\frac{\mu^2}{2}-B^2\right)\sin\Psi\\
&+\beta_{1c}\gamma\frac{B^3}{6}\mu\cos(2\Psi)+\left(\beta_{1s}\gamma\frac{B^3}{6}\mu+\beta_0\gamma\frac{B^2}{8}\mu^2\right)\sin(2\Psi)\\
&-\beta_{1s}\gamma\frac{B^2}{16}\mu^2\cos(3\Psi)+\beta_{1c}\gamma\frac{B^2}{16}\mu^2\sin(3\Psi)=\\
&=\left[\frac{\gamma}{2}\left(\frac{B^3}{3}\lambda-\frac{B^3}{6}\frac{p_{cw}}{\Omega_R}\mu+\frac{B^4}{4}\theta+\frac{B^2}{4}\theta\mu^2\right)-\frac{gS_B}{J_B\Omega_R^2}\right]\\
&+\left[\frac{\gamma}{2}\left(\frac{B^4}{4}\frac{q_{cw}}{\Omega_R}-\beta_0\frac{B^3}{3}\mu\right)-2\frac{p_{cw}}{\Omega_R}\right]\cos\Psi\\
&+\left[\frac{\gamma}{2}\left(-\frac{B^4}{4}\frac{p_{cw}}{\Omega_R}+\frac{B^2}{2}\lambda\mu+\frac{2}{3}B^3\theta\mu\right)-2\frac{q_{cw}}{\Omega_R}\right]\sin\Psi\\
&+\left[\frac{\gamma}{2}\left(\frac{B^3}{6}\frac{p_{cw}}{\Omega_R}\mu-\frac{B^2}{4}\theta\mu^2\right)\right]\cos(2\Psi)\\
&+\left[\frac{\gamma}{2}\left(\frac{B^3}{6}\frac{q_{cw}}{\Omega_R}\mu\right)\right]\sin(2\Psi)
\end{aligned}\tag{2.197}$$

Neglecting all blade flapping harmonics above the first [16] equations (2.196) and (2.197) can be simplified as follows.

$$\begin{aligned}
&\beta_0+\beta_{1s}\gamma\frac{B^2}{8}\left(\frac{\mu^2}{2}+B^2\right)\cos\Psi+\beta_{1c}\gamma\frac{B^2}{8}\left(\frac{\mu^2}{2}-B^2\right)\sin\Psi=\\
&=\left[\frac{\gamma}{2}\left(\frac{B^3}{3}\lambda+\frac{B^3}{6}\frac{p_{cw}}{\Omega_R}\mu+\frac{B^4}{4}\theta+\frac{B^2}{4}\theta\mu^2\right)-\frac{g\,S_B}{J_B\Omega_R^2}\right]\\
&\quad+\left[\frac{\gamma}{2}\left(\frac{B^4}{4}\frac{q_{cw}}{\Omega_R}-\frac{B^3}{3}\beta_0\mu\right)+2\frac{p_{cw}}{\Omega_R}\right]\cos\Psi\\
&\quad+\left[\frac{\gamma}{2}\left(\frac{B^4}{4}\frac{p_{cw}}{\Omega_R}+\frac{B^2}{2}\lambda\mu+\frac{2}{3}B^3\theta\mu\right)-2\frac{q_{cw}}{\Omega_R}\right]\sin\Psi
\end{aligned} \tag{2.198}$$

$$\begin{aligned}
&\beta_0+\beta_{1s}\gamma\frac{B^2}{8}\left(\frac{\mu^2}{2}+B^2\right)\cos\Psi+\beta_{1c}\gamma\frac{B^2}{8}\left(\frac{\mu^2}{2}-B^2\right)\sin\Psi=\\
&=\left[\frac{\gamma}{2}\left(\frac{B^3}{3}\lambda-\frac{B^3}{6}\frac{p_{cw}}{\Omega_R}\mu+\frac{B^4}{4}\theta+\frac{B^2}{4}\theta\mu^2\right)-\frac{g\,S_B}{J_B\Omega_R^2}\right]\\
&\quad+\left[\frac{\gamma}{2}\left(\frac{B^4}{4}\frac{q_{cw}}{\Omega_R}-\beta_0\frac{B^3}{3}\mu\right)-2\frac{p_{cw}}{\Omega_R}\right]\cos\Psi\\
&\quad+\left[\frac{\gamma}{2}\left(-\frac{B^4}{4}\frac{p_{cw}}{\Omega_R}+\frac{B^2}{2}\lambda\mu+\frac{2}{3}B^3\theta\mu\right)-2\frac{q_{cw}}{\Omega_R}\right]\sin\Psi
\end{aligned} \tag{2.199}$$

Equations (2.198) and (2.199) can be transformed to get blade flapping coefficients:

– for counterclockwise direction of rotor

$$\beta_0=\frac{\gamma}{2}\left(\frac{B^3}{3}\lambda+\frac{B^3}{6}\frac{p_{cw}}{\Omega_R}\mu+\frac{B^4}{4}\theta+\frac{B^2}{4}\theta\mu^2\right)-\frac{g\,S_B}{J_B\Omega_R^2} \tag{2.200}$$

$$\beta_{1c}=2\mu\left(\lambda+\frac{4}{3}B\,\theta\right)\frac{1}{\left(\frac{\mu^2}{2}-B^2\right)}+\left(B^4\frac{p_{cw}}{\Omega_R}-16\frac{q_{cw}}{\gamma\Omega_R}\right)\frac{1}{B^2\left(\frac{\mu^2}{2}-B^2\right)} \tag{2.201}$$

$$\beta_{1s}=-\frac{4}{3}\beta_0\mu\frac{B}{\left(\frac{\mu^2}{2}+B^2\right)}+\left(B^4\frac{q_{cw}}{\Omega_R}+16\frac{p_{cw}}{\gamma\Omega_R}\right)\frac{1}{B^2\left(\frac{\mu^2}{2}+B^2\right)} \tag{2.202}$$

– for clockwise direction of rotor

$$\beta_0 = \frac{\gamma}{2}\left(\frac{B^3}{3}\lambda - \frac{B^3}{6}\frac{p_{cw}}{\Omega_R}\mu + \frac{B^4}{4}\theta + \frac{B^2}{4}\theta\mu^2\right) - \frac{g\,S_B}{J_B\Omega_R^2} \tag{2.203}$$

$$\beta_{1c} = 2\mu\left(\lambda + \frac{4}{3}B\,\theta\right)\frac{1}{\left(\frac{\mu^2}{2} - B^2\right)} - \left(B^4\frac{p_{cw}}{\Omega_R} + 16\frac{q_{cw}}{\gamma\Omega_R}\right)\frac{1}{B^2\left(\frac{\mu^2}{2} - B^2\right)} \tag{2.204}$$

$$\beta_{1s} = -\frac{4}{3}\beta_0\mu\frac{B}{\left(\frac{\mu^2}{2} + B^2\right)} + \left(B^4\frac{q_{cw}}{\Omega_R} - 16\frac{p_{cw}}{\gamma\Omega_R}\right)\frac{1}{B^2\left(\frac{\mu^2}{2} + B^2\right)} \tag{2.205}$$

2.6. Landing Gear

Contact Point

Landing gear contact point is considered to be an intersection of the ground plane and the line segment with the beginning at the strut attachment point and the end at the tire bottom.

Intersection of a line segment and a plane can be calculated using following expression. [20]

$$u = \frac{\vec{n}\cdot\left(\vec{r}_p - \vec{r}_b\right)}{\vec{n}\cdot\left(\vec{r}_e - \vec{r}_b\right)} \tag{2.206}$$

where

$\vec{n}$ – unit vector normal to the plane

$\vec{r}_b$ – position vector of the line segment beginning

$\vec{r}_e$ – position vector of the line segment end

$\vec{r}_p$ – position vector of any point on the plane

u – normalize coordinate of intersection point along line segment

If $0 \leqslant u \leqslant 1$ then intersection point is within line segment and its coordinates are given by the following formula.

$$\vec{r} = \vec{r}_b + u\left(\vec{r}_e - \vec{r}_b\right) \tag{2.207}$$

If denominator of expression (2.206) is zero then the line segment is parallel to the plane. If both numerator and denominator are zero then the line segment lies on the plane.

Forces and Moments

Forces generated by the landing gear can be divided into:

– normal to the ground plane forces due to struts and tires deflection,

– tangent to the ground plane forces due to friction between tires and the ground.

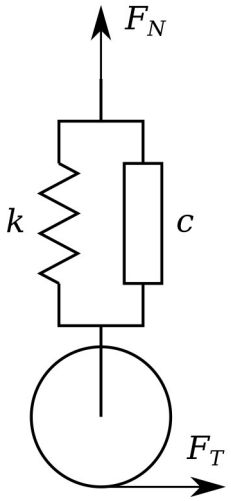

Figure 2-8: Landing gear forces

Normal forces are the sum of forces due to spring and damper while tangent force are caused by static or kinetic friction and optional rolling friction and are given as follows. [21]

$$F_N = kx + c\dot{x} \tag{2.208}$$

$$F_T = \mu F_N \tag{2.209}$$

Surface	**Static friction coefficient**	**Kinetic friction coefficient**
Concrete (dry)	0.8 – 1.0	0.7 – 0.8
Concrete (wet)	0.6 – 0.8	0.5 – 0.6
Tarmac (dry)	0.7 – 0.8	0.6 – 0.7
Tarmac (wet)	0.4 – 0.5	0.3 – 0.4
Dirt (dry)	0.5 – 0.6	0.2 – 0.3
Dirt (wet)	0.3 – 0.4	0.2 – 0.3
Snow	0.1 – 0.4	0.2 – 0.3
Ice	0.05 – 0.15	0.05 – 0.10

Table 2-3: Static and kinetic friction coefficients [22]

Surface	Rolling friction coefficient
Tarmac	0.010 – 0.012
Concrete	0.012 – 0.015
Dirt	0.030 – 0.140

Table 2-4: Rolling friction coefficients [22]

2.7. Mass and Inertia

Empty Aircraft Moments of Inertia

Aircraft is divided into structure groups which mass is estimated. This groups are assumed to be homogeneous rigid body with simple shape which allows to calculate its moment of inertia using an exact closed-form expression, given e.g. in [23].

Steiner's theorem, given by the following expression, is used to express aircraft structure groups inertia tensor in Body Axis System. [5, 21]

$$\boldsymbol{I}_b = \boldsymbol{I}_0 + m\begin{bmatrix} y^2+z^2 & -xy & -xz \\ -yx & x^2+z^2 & -yz \\ -zx & -zy & x^2+y^2 \end{bmatrix} \tag{2.210}$$

Sum of all aircraft structure groups inertia tensors gives empty aircraft inertia tensor.

$$\boldsymbol{I}_b = \sum_j \boldsymbol{I}_{j,b} \tag{2.211}$$

Variable Masses

All variable masses, crew, fuel, payload, etc., are considered to be point masses. Point mass inertia tensor can be calculated using formula (2.210), where $\boldsymbol{I}_0 = 0$. This tensors are then added to the empty aircraft inertia tensor giving total aircraft inertia tensor.

Aircraft total first moment of mass is given as follows.

$$\vec{S}_b = \sum_j m_j \vec{r}_{CM,j,b} \tag{2.212}$$

Position of aircraft center of mass including variable masses is then given by following formula.

$$\vec{r}_{CM,b} = \frac{\vec{S}_b}{\sum_j m_j} \tag{2.213}$$

2.8. Propulsion

2.8.1. Piston Engine

Piston engine manifold absolute pressure, expressed in pascals, is given by the following formula [8]. Engine revolution speed RPM is expressed in revolutions per minute.

$$MAP = p(h) + \left(156.9411\,\hat{\delta}_{throttle} - 158.8034\right) RPM \tag{2.214}$$

Fuel to air ratio is approximated by the following expression. [8]

$$FAR = 0.1\left(2 - \hat{\delta}^2_{mixture}\right)\frac{\rho_0}{\rho} \tag{2.215}$$

Static power, expressed in watts, is given as follows. [8]

$$P_S = P_{max} MAP\left(7.198759595625\cdot 10^{-9} RPM - 1.84583579375\cdot 10^{-6}\right) \tag{2.216}$$

Power losses, expressed in watts, can be calculated using following formula. [8]

$$\Delta P = P_{max} 2.58125\cdot 10^{-4}\frac{RPM^2}{2700} \tag{2.217}$$

Engine net power, expressed in watts, is given by the following formula. [8]

$$P_N = P_S F_P - \Delta P \tag{2.218}$$

where power factor F_P is a function of fuel to air ration given in [8].

2.8.2. Propeller

Thrust generated by the propeller and power required by the propeller are given by the following equations. [8, 24] Propeller revolution speed *n* is expressed in revolutions per second.

$$T = \rho n^2 D^4 C_T \tag{2.219}$$

$$P = \rho n^3 D^5 C_P \tag{2.220}$$

where thrust C_T and power C_P coefficients are functions of advance ratio and blade angle and they can be found in [25].

Advance ratio is given by the following formula. [8, 24, 26]

$$J = \frac{V}{nD} \tag{2.221}$$

The propeller torque required is given as. [21]

$$Q = \frac{P}{2\pi n} \tag{2.222}$$

3. Automatic Flight Control Systems

3.1. Common Control Systems Elements

Characteristics and properties of common control systems elements are given below. [27, 28]

3.1.1. Proportional Element – P

Figure 3-1: Proportional element block diagram

Proportional element time domain differential equation ans s-domain transfer function are given as follows:

$$y(t)=k\,u(t) \tag{3.1}$$

$$G(s)=k \tag{3.2}$$

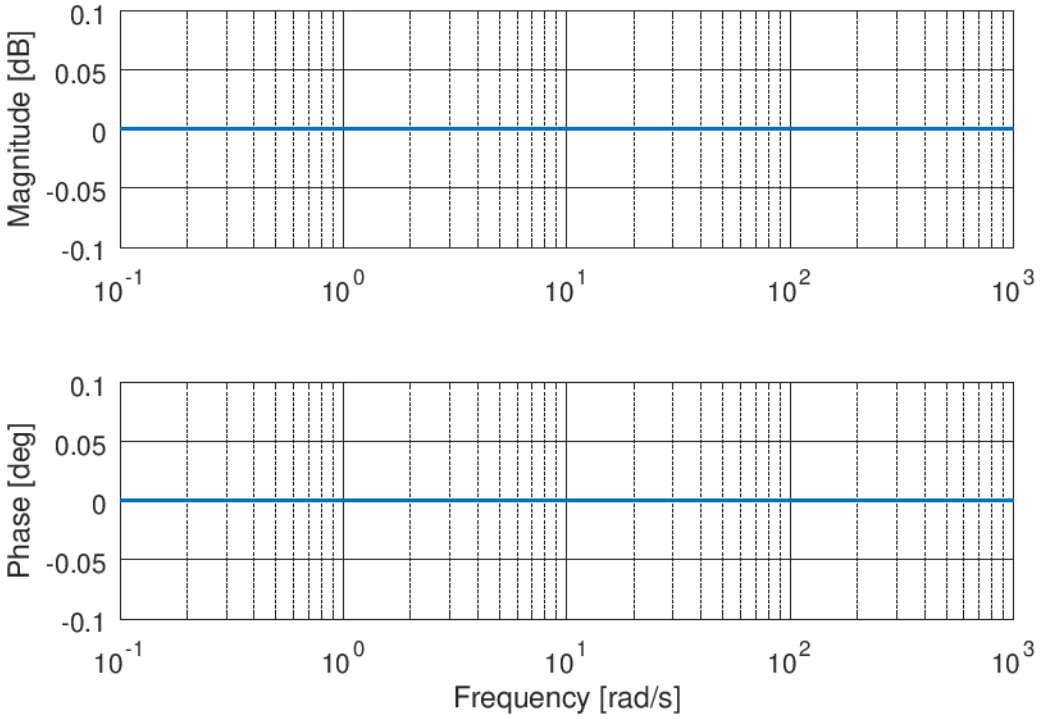

Figure 3-2: Proportional element Bode diagram

3.1.2. Integrator (ideal) – I

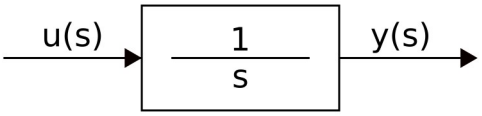

Figure 3-3: Ideal integrator block diagram

Time domain differential equation ans s-domain transfer function are given as follows:

$$\frac{dy}{dt} = u(t) \tag{3.3}$$

$$G(s) = \frac{1}{s} \tag{3.4}$$

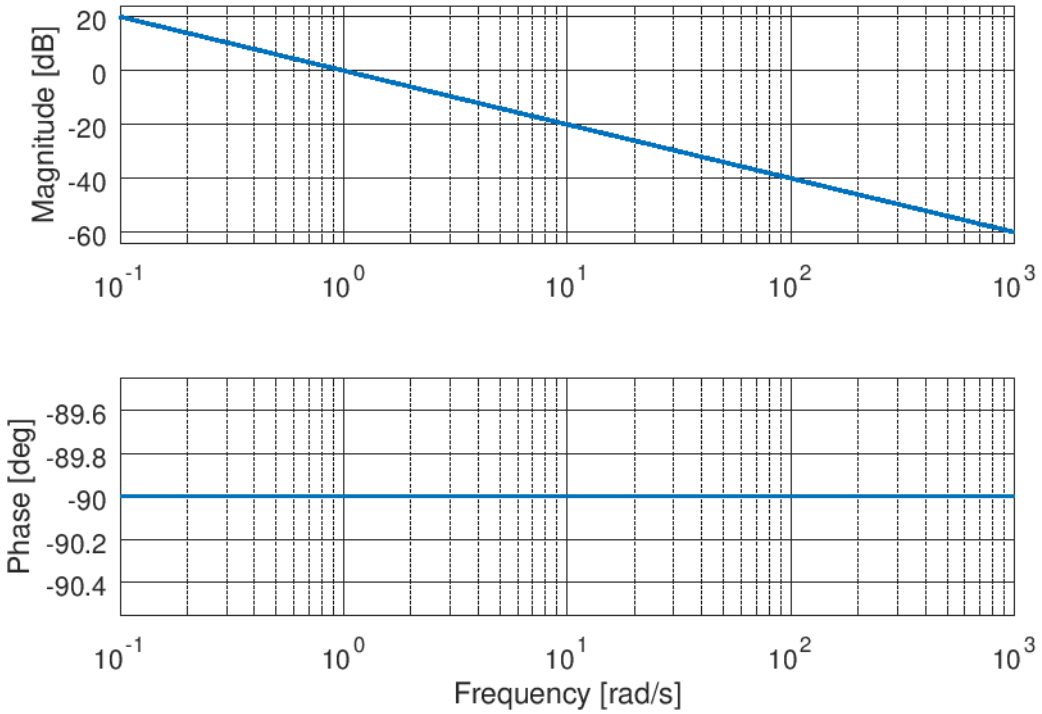

Figure 3-4: Ideal integrator Bode diagram

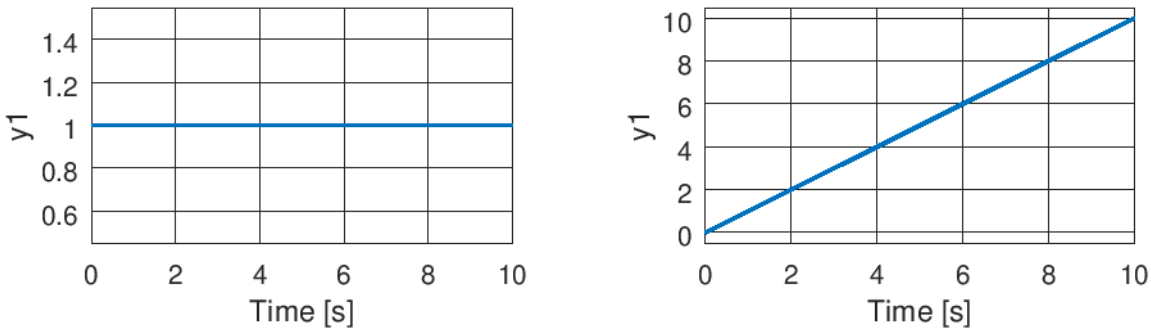

Figure 3-5: Ideal integrator impulse and step response

3.1.3. Differentiator (ideal) – D

Figure 3-6: Ideal differentiator block diagram

Ideal differentiator time domain differential equation ans s-domain transfer function are given as follows:

$$y(t)=\frac{du}{dt} \tag{3.5}$$

$$G(s)=s \tag{3.6}$$

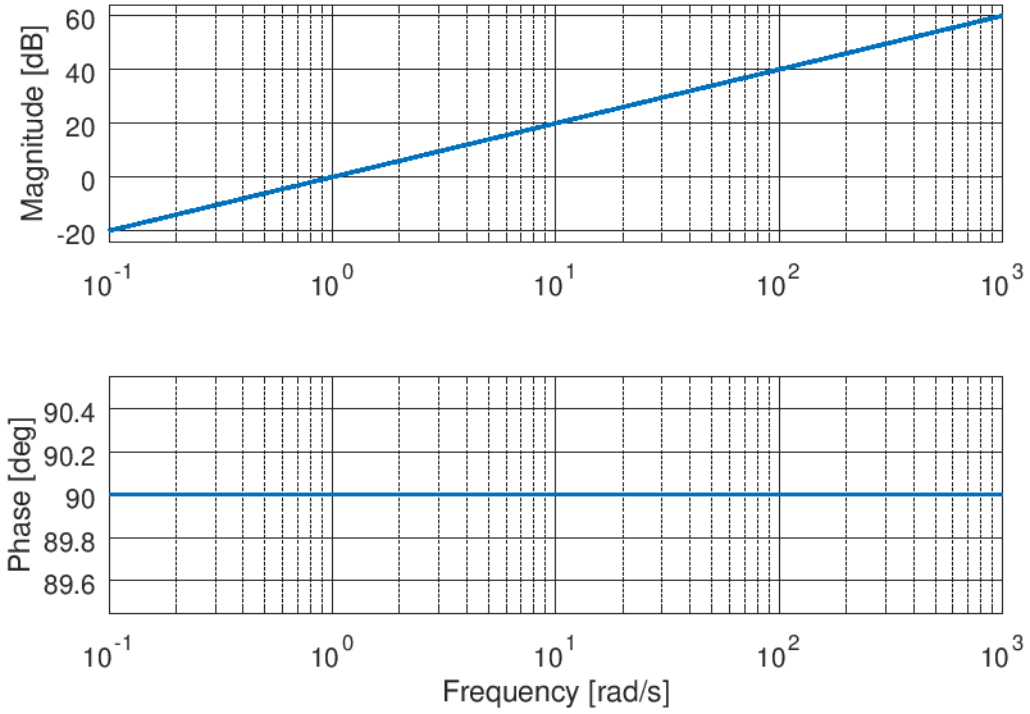

Figure 3-7: Ideal differentiator Bode diagram

3.1.4. First-Order Lead

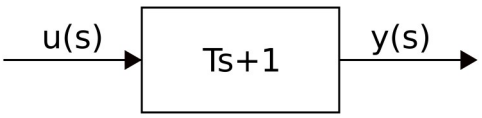

Figure 3-8: First-order lead block diagram

First-order lead time domain differential equation ans s-domain transfer function are given as follows:

$$y(t) = T\frac{du}{dt} + u(t) \tag{3.7}$$

$$G(s) = Ts + 1 \tag{3.8}$$

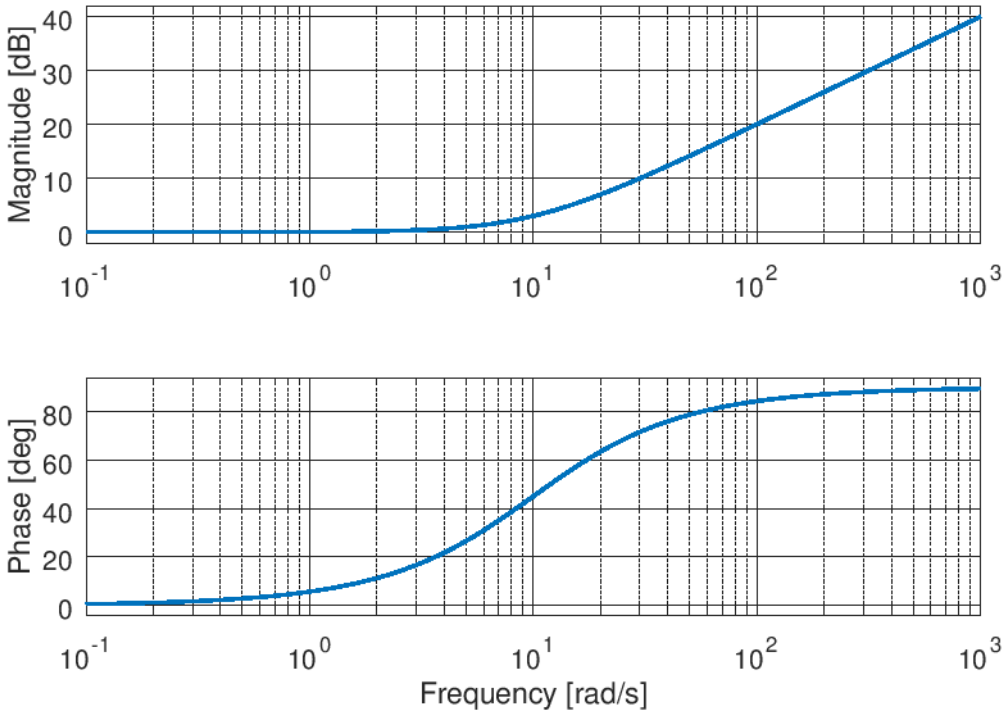

Figure 3-9: First-order lead Bode diagram

3.1.5. First-Order Lag

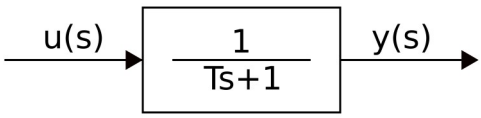

Figure 3-10: First-order lag block diagram

Time domain differential equation ans s-domain transfer function are given as follows:

$$T\frac{dy}{dt}+y(t)=u(t) \tag{3.9}$$

$$G(s)=\frac{1}{Ts+1} \tag{3.10}$$

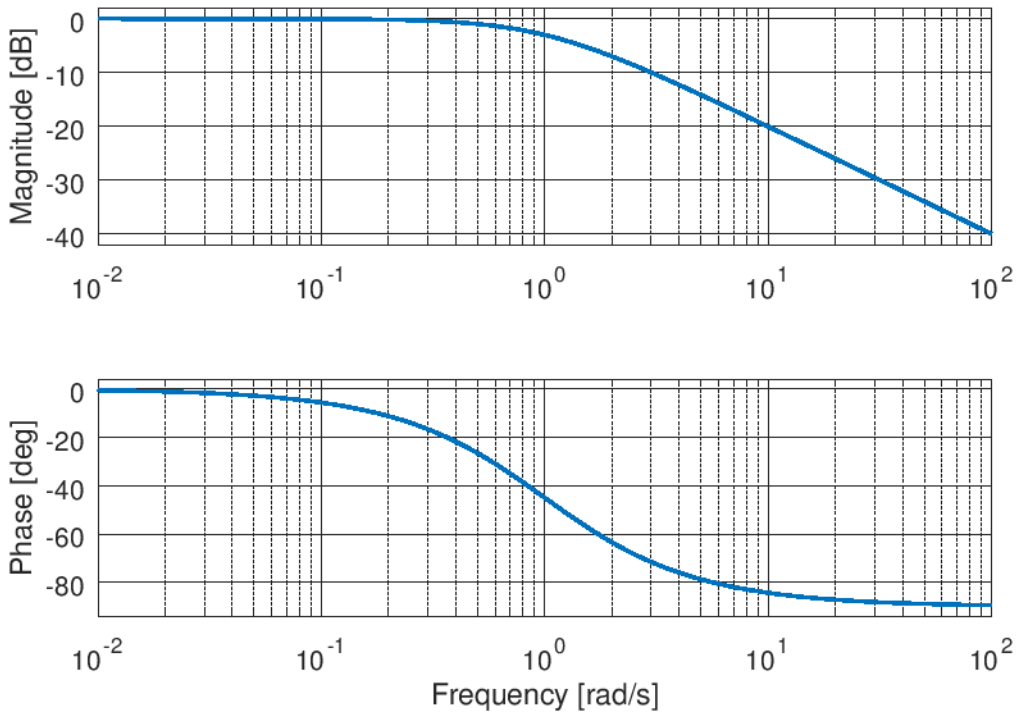

Figure 3-11: First-order lag Bode diagram

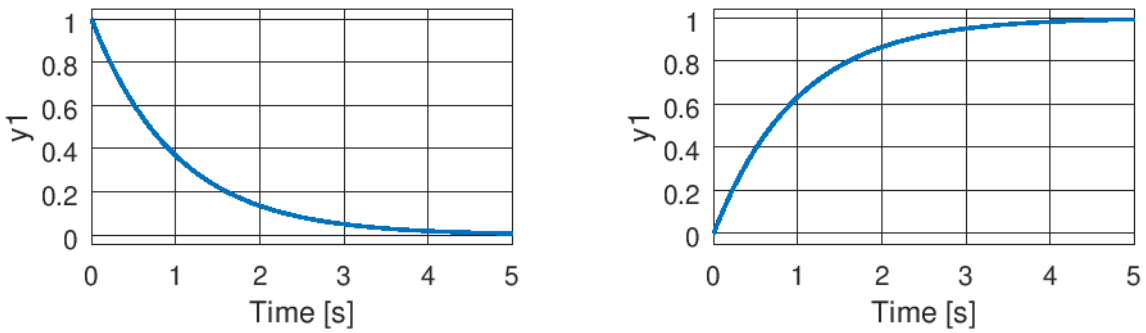

Figure 3-12: First-order lag impulse and step response

3.1.6. Integrator (real)

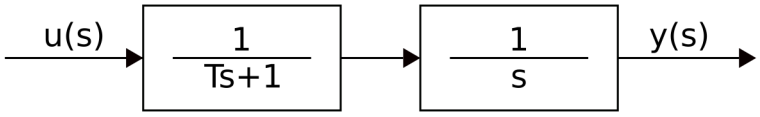

Figure 3-13: Real integrator block diagram

Time domain differential equation ans s-domain transfer function are given as follows:

$$T\frac{d^2y}{dt^2}+\frac{dy}{dt}=1\,u(t) \tag{3.11}$$

$$G(s)=\frac{1}{s(Ts+1)} \tag{3.12}$$

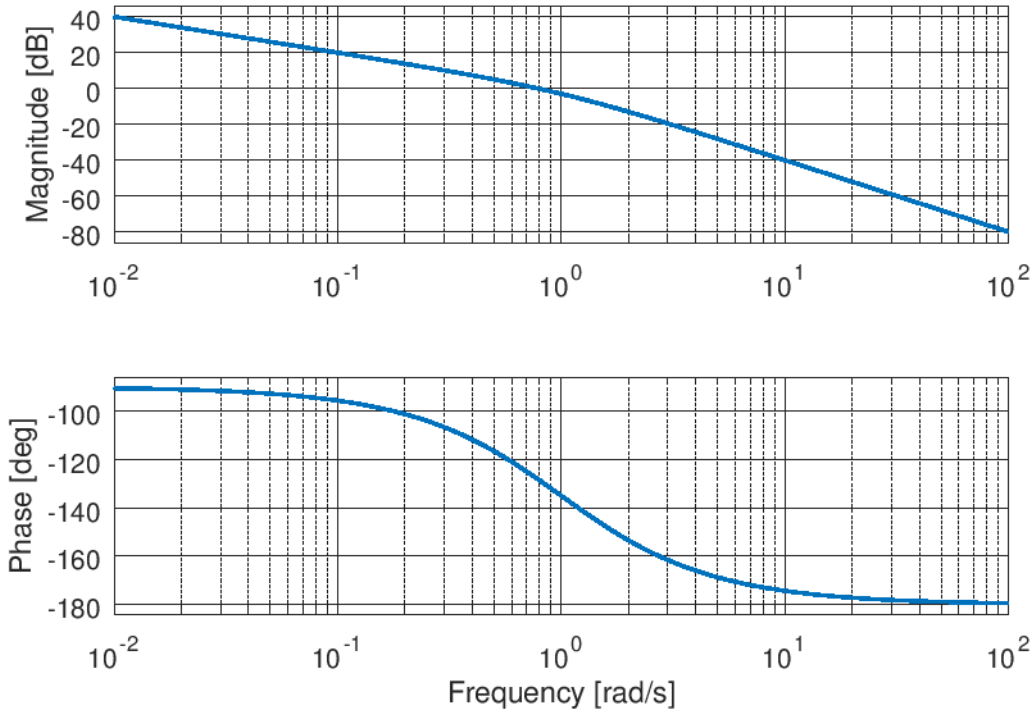

Figure 3-14: Real integrator Bode diagram

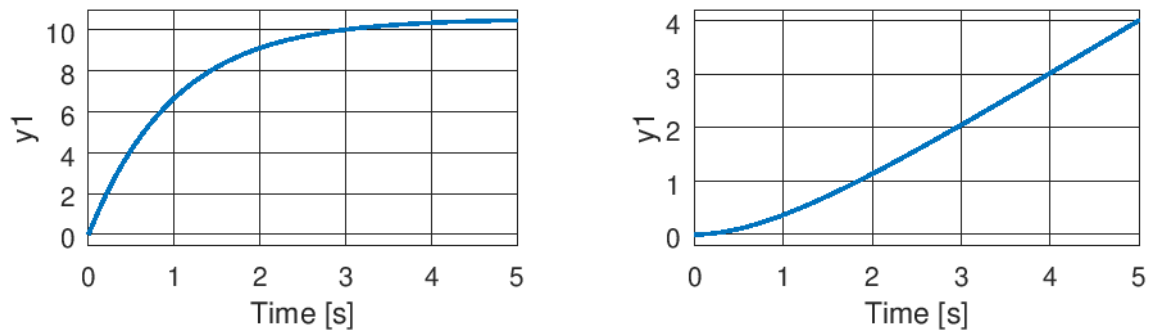

Figure 3-15: Real integrator impulse and step response

3.1.7. Differentiator (real)

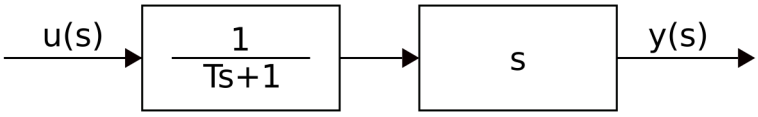

Figure 3-16: Real differentiator block diagram

Time domain differential equation ans s-domain transfer function are given as follows:

$$T\frac{dy}{dt}+y(t)=\frac{du}{dt} \tag{3.13}$$

$$G(s)=\frac{s}{Ts+1} \tag{3.14}$$

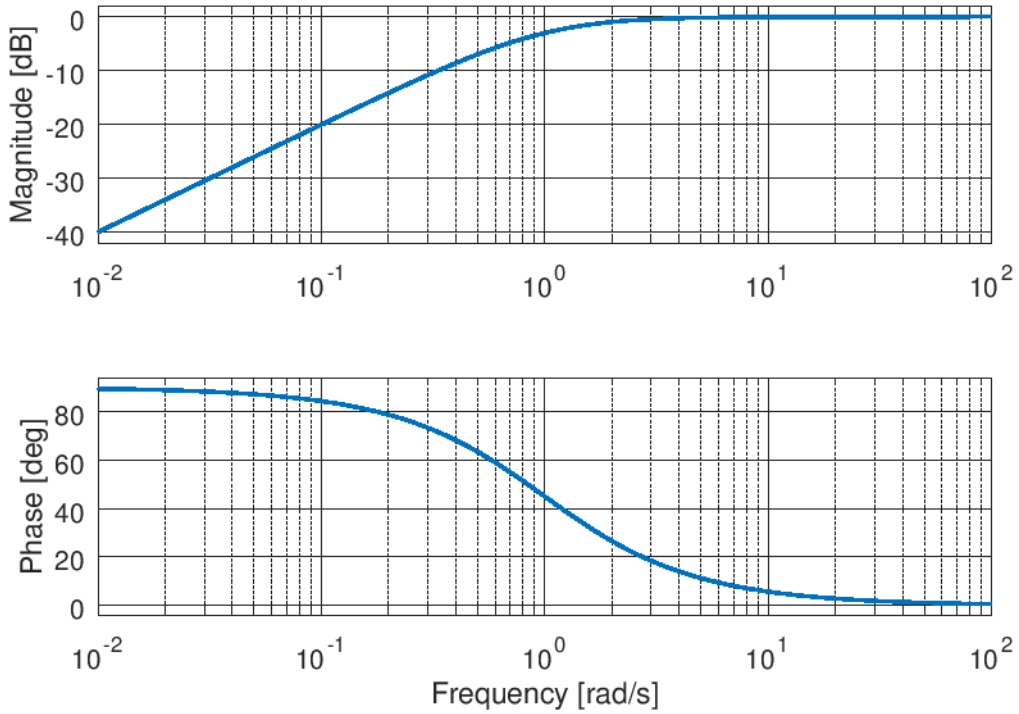

Figure 3-17: Real differentiator Bode diagram

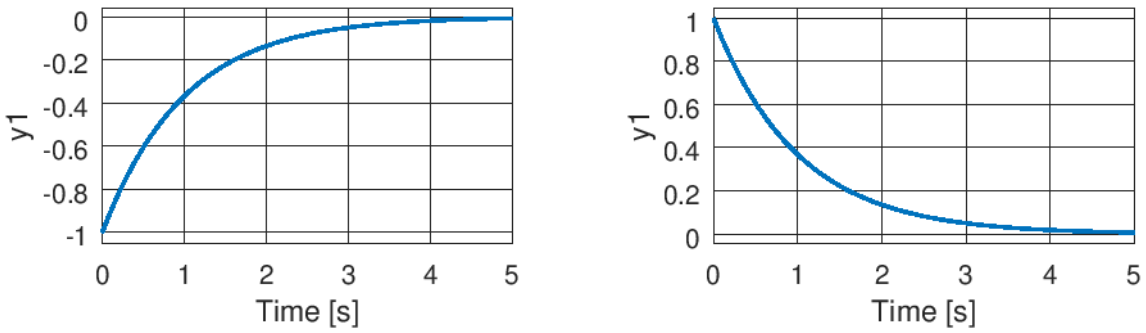

Figure 3-18: Real differentiator impulse and step response

3.1.8. Second-Order Lag

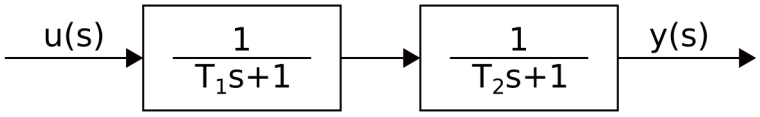

Figure 3-19: Second-order lag block diagram

Time domain differential equation ans s-domain transfer function are given as follows:

$$T_1 T_2 \frac{d^2 y}{dt^2} + (T_1 + T_2)\frac{dy}{dt} + y(t) = u(t) \tag{3.15}$$

$$G(s) = \frac{1}{(T_1 s + 1)(T_2 s + 1)} \tag{3.16}$$

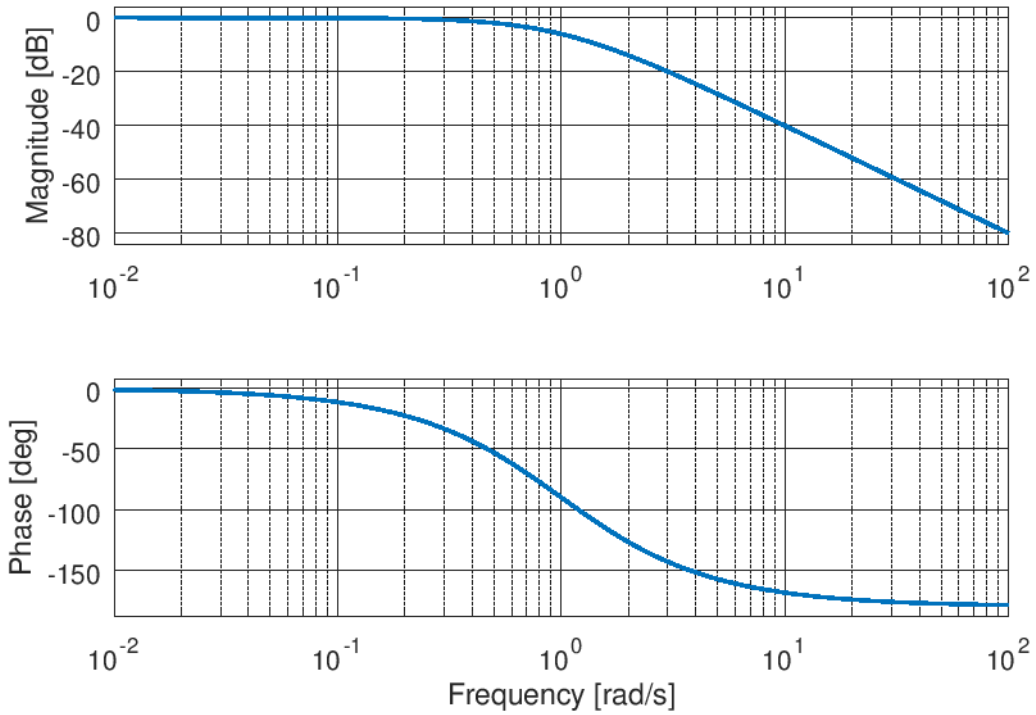

Figure 3-20: Second-order lag Bode diagram

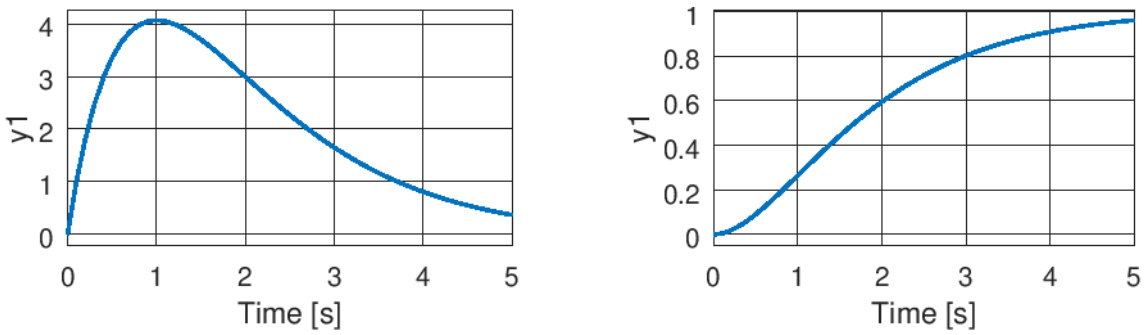

Figure 3-21: Second-order lag impulse and step response

3.1.9. Low-Pass Filter

First-order lag is a low-pass filter

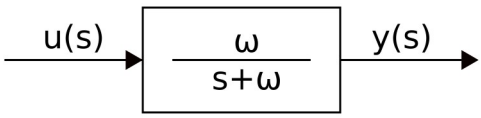

Figure 3-22: Low-pass filter block diagram

Low-pass filter time domain differential equation ans s-domain transfer function are given as follows:

$$\frac{1}{\omega}\frac{dy}{dt}+y(t)=\frac{1}{\omega}u(t) \tag{3.17}$$

$$G(s)=\frac{\omega}{s+\omega} \tag{3.18}$$

3.1.10. High-Pass (Washout) Filter

Real differentiator is a high-pass filter.

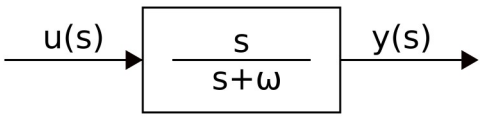

Figure 3-23: High-pass filter block diagram

High-pass filter time domain differential equation ans s-domain transfer function are given as follows:

$$\frac{1}{\omega}\frac{dy}{dt}+y(t)=\frac{1}{\omega}\frac{du}{dt} \tag{3.19}$$

$$G(s)=\frac{s}{s+\omega} \tag{3.20}$$

3.1.11. Lead-Lag Compensator

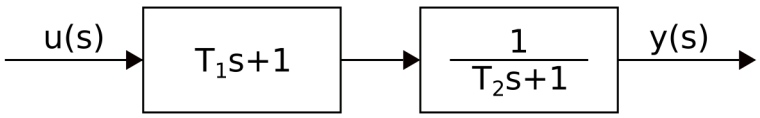

Figure 3-24: Lead-lag compensator block diagram

Lead-lag compensator s-domain transfer function are given as follows:

$$G(s)=\frac{(T_1 s+1)}{(T_2 s+1)} \tag{3.21}$$

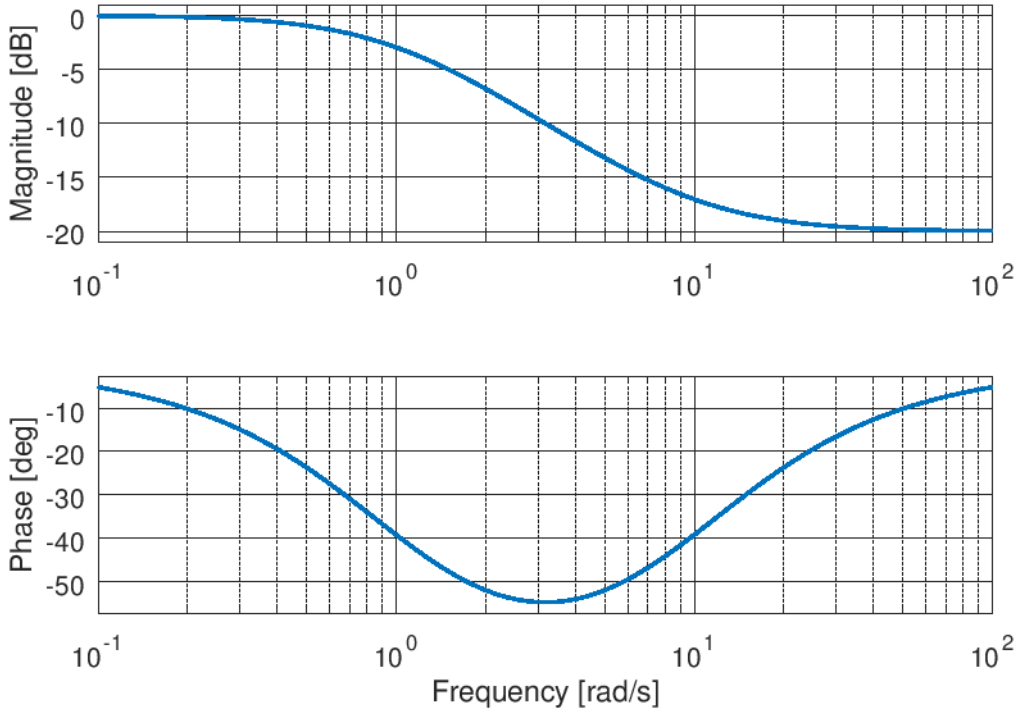

Figure 3-25: Lead-lag compensator Bode diagram

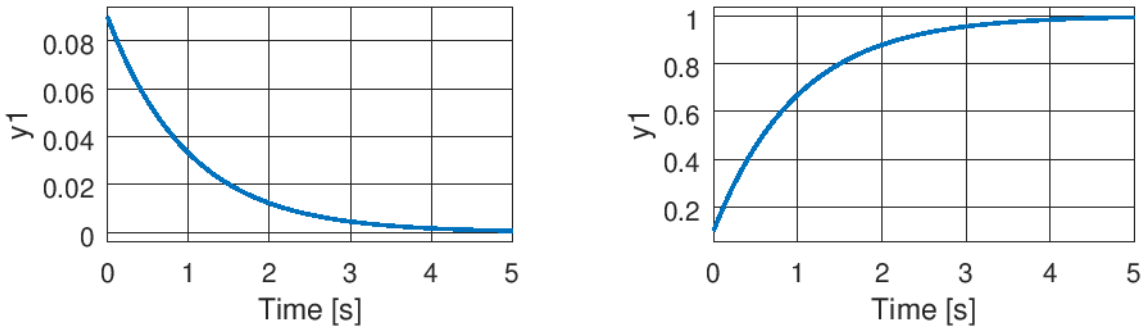

Figure 3-26: Lead-lag compensator impulse and step response

3.1.12. PID Controller

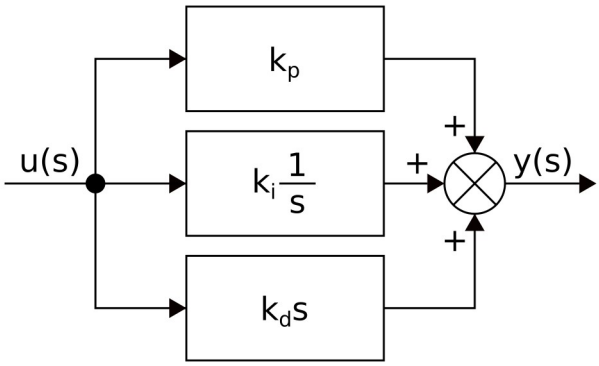

Figure 3-27: PID controller block diagram

PID controller s-domain transfer function are given as follows:

$$G(s) = k_p + k_i \frac{1}{s} + k_d s \tag{3.22}$$

4. Obtaining Data

4.1. Aerodynamic Characteristics

4.1.1. Aerodynamic Characteristics Approximation

Following approximation is used to get lift coefficient for the full range of angle of attack. [29]

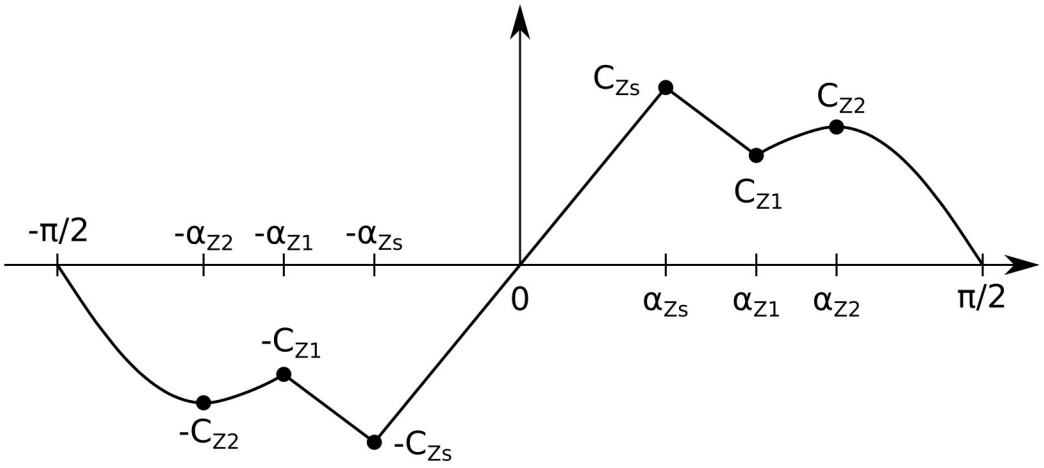

Figure 4-1: Lift coefficient approximation

Lift coefficient is given by the following expressions.

$$C_Z=\frac{-(\alpha+\alpha_{Z2})\left(\alpha+\frac{\pi}{2}\right)}{(\alpha_{Z1}-\alpha_{Z2})\left(\alpha_{Z1}-\frac{\pi}{2}\right)}C_{Z1}-\frac{(\alpha+\alpha_{Z1})\left(\alpha+\frac{\pi}{2}\right)}{(\alpha_{Z2}-\alpha_{Z1})\left(\alpha_{Z2}-\frac{\pi}{2}\right)}C_{Z2}\text{, for } -\frac{\pi}{2}\leqslant\alpha\leqslant-\alpha_{Z1} \tag{4.1}$$

$$C_Z=\frac{C_{Z1}-C_{Zs}}{\alpha_{Z1}-\alpha_{Zs}}(\alpha+\alpha_{Zs})-C_{Zs}\text{, for } -\alpha_{Z1}<\alpha\leqslant-\alpha_{Zs} \tag{4.2}$$

$$C_Z=\frac{C_{Zs}}{\alpha_{Zs}}\alpha\text{, for } -\alpha_{Zs}<\alpha<\alpha_{Zs} \tag{4.3}$$

$$C_Z=\frac{C_{Z1}-C_{Zs}}{\alpha_{Z1}-\alpha_{Zs}}(\alpha-\alpha_{Zs})+C_{Zs}\text{, for } \alpha_{Zs}\leqslant\alpha<\alpha_{Z1} \tag{4.4}$$

$$C_Z=\frac{(\alpha-\alpha_{Z2})\left(\alpha-\frac{\pi}{2}\right)}{(\alpha_{Z1}-\alpha_{Z2})\left(\alpha_{Z1}-\frac{\pi}{2}\right)}C_{Z1}+\frac{(\alpha-\alpha_{Z1})\left(\alpha-\frac{\pi}{2}\right)}{(\alpha_{Z2}-\alpha_{Z1})\left(\alpha_{Z2}-\frac{\pi}{2}\right)}C_{Z2}\text{, for } \alpha_{Z1}\leqslant\alpha\leqslant\frac{\pi}{2} \tag{4.5}$$

Following approximation is used to get drag coefficient for the full range of angle of attack. [29] Drag coefficient is assumed to be symmetric.

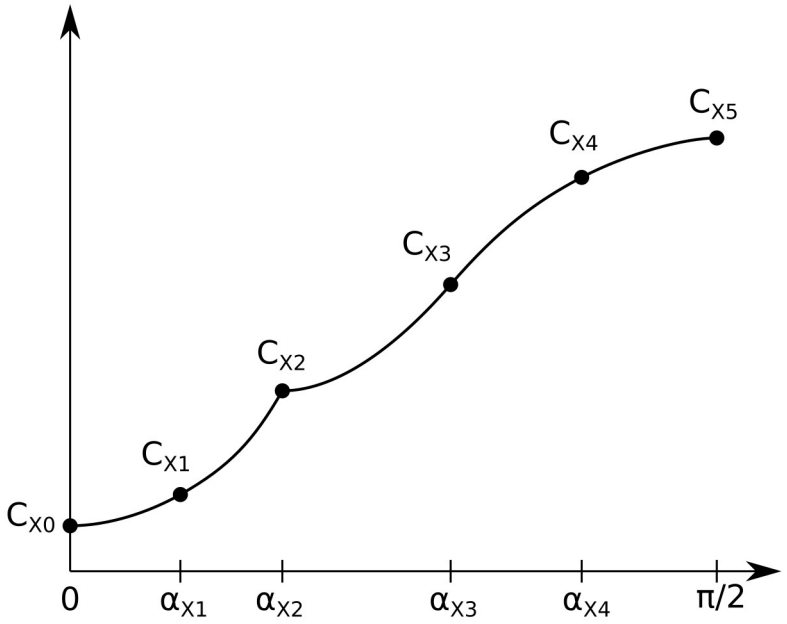

Figure 4-2: Drag coefficient approximation

Drag coefficient is given by the following expressions.

$$C_X = \frac{\left(\alpha^2-\alpha_{X2}^2\right)\left(\alpha^2-\alpha_{X1}^2\right)}{\alpha_{X1}^2\alpha_{X2}^2}C_{X0} + \frac{\left(\alpha^2-\alpha_{X2}^2\right)\alpha^2}{\left(\alpha_{X1}^2-\alpha_{X2}^2\right)\alpha_{X1}^2}C_{X1} + \frac{\left(\alpha^2-\alpha_{X1}^2\right)\alpha^2}{\left(\alpha_{X2}^2-\alpha_{X1}^2\right)\alpha_{X2}^2}C_{X2}, \quad \text{for } -\alpha_{X2} \leqslant \alpha \leqslant \alpha_{X2} \tag{4.6}$$

$$C_X = \frac{(\alpha-\alpha_{X3})(\alpha-\alpha_{X4})\left(\alpha-\frac{\pi}{2}\right)}{(\alpha_{X2}-\alpha_{X3})(\alpha_{X2}-\alpha_{X4})\left(\alpha_{X2}-\frac{\pi}{2}\right)}C_{X2} + \frac{(\alpha-\alpha_{X2})(\alpha-\alpha_{X4})\left(\alpha-\frac{\pi}{2}\right)}{(\alpha_{X3}-\alpha_{X2})(\alpha_{X3}-\alpha_{X4})\left(\alpha_{X3}-\frac{\pi}{2}\right)}C_{X3} + \frac{(\alpha-\alpha_{X2})(\alpha-\alpha_{X3})\left(\alpha-\frac{\pi}{2}\right)}{(\alpha_{X4}-\alpha_{X2})(\alpha_{X4}-\alpha_{X3})\left(\alpha_{X4}-\frac{\pi}{2}\right)} + C_{X4}\frac{(\alpha-\alpha_{X2})(\alpha-\alpha_{X3})(\alpha-\alpha_{X4})}{\left(\frac{\pi}{2}-\alpha_{X2}\right)\left(\frac{\pi}{2}-\alpha_{X3}\right)\left(\frac{\pi}{2}-\alpha_{X4}\right)}C_{X5}, \quad \text{for } -\alpha_{X2} \leqslant \alpha \leqslant \alpha_{X2} \tag{4.7}$$

Data available in [30] and [31] can be used to approximate aerodynamic characteristics outside linear range of the lift..

4.1.2. Half-Wing Aerodynamic Center Coordinates

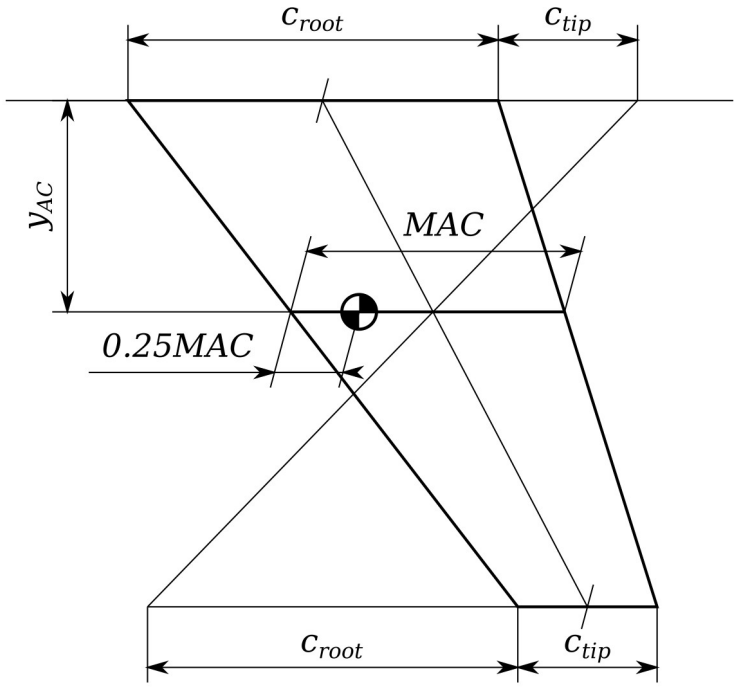

Figure 4-3: Half-wing aerodynamic center

Position of half-wing aerodynamic center $\vec{r}_{AC}$ is at 25% of the mean aerodynamic chord and its lateral coordinate is given by the following formula. [24, 26]

$$y_{AC} = \frac{b(1+2\lambda)}{6(1+\lambda)} \tag{4.8}$$

where taper ratio λ is given by the following formula. [24]

$$\lambda = \frac{c_{tip}}{c_{root}} \tag{4.9}$$

4.1.3. Horizontal Tail Incidence

Equilibrium of moments acting on an aircraft is given by the following equation.

$$r_{CG} mg + \frac{1}{2}\rho V^2 S \hat{c} C_m = l_h \frac{1}{2}\rho V^2 S_h C_{Z,h} \tag{4.10}$$

Horizontal stabilizer lift coefficient is given as follows.

$$C_{Z,h} = \left(\alpha + i_h - \alpha\frac{\partial \epsilon}{\partial \alpha}\right)\frac{dC_{Z,h}}{d\alpha} \tag{4.11}$$

Substituting equation (4.11) into (4.10) gives

$$r_{CG} mg + \frac{1}{2}\rho V^2 S \hat{c} C_m = l_h \frac{1}{2}\rho V^2 S_h \left(\alpha + i_h - \alpha \frac{\partial \epsilon}{\partial \alpha} \right) \frac{dC_{Z,h}}{d\alpha} \tag{4.12}$$

Solving this equation for horizontal tail incidence angle gives

$$i_h = \frac{2 r_{CG} mg + \rho V^2 S \hat{c} C_m}{l_h \rho V^2 S_h \frac{dC_{Z,h}}{d\alpha}} - \alpha \left(1 - \frac{\partial \epsilon}{\partial \alpha} \right) \tag{4.13}$$

Equilibrium of forces acting on an aircraft in level flight is given by the following equation.

$$mg = \frac{1}{2}\rho V^2 S C_Z \tag{4.14}$$

Aircraft lift coefficient is given as follows.

$$C_Z = C_{Z0} + \alpha \frac{dC_Z}{d\alpha} \tag{4.15}$$

Substituting equation (4.15) into (4.14) gives

$$mg = \frac{1}{2}\rho V^2 S \left(C_{Z0} + \alpha \frac{dC_Z}{d\alpha} \right) \tag{4.16}$$

Solving this equation for angle of attack gives

$$\alpha = \frac{2mg - \rho V^2 S C_{Z0}}{\rho V^2 S \frac{dC_Z}{d\alpha}} \tag{4.17}$$

Substituting equation (4.17) into (4.13) gives

$$i_h = \frac{2 r_{CG} mg + \rho V^2 S \hat{c} C_m}{l_h \rho V^2 S_h \frac{dC_{Z,h}}{d\alpha}} - \frac{2mg - \rho V^2 S C_{Z0}}{\rho V^2 S \frac{dC_Z}{d\alpha}} \left(1 - \frac{\partial \epsilon}{\partial \alpha} \right) \tag{4.18}$$

4.1.4. Critical Angle of Attack

Equilibrium of forces acting on an aircraft in level flight is given by the following equation.

$$mg = \frac{1}{2}\rho V^2 \left(S C_Z + S_h C_{Z,h} \right) \tag{4.19}$$

As conventional configuration airplanes have horizontal stabilizer negative incidence angle, it is assumed that horizontal stabilizer is within its lift linear range when maximum lift coefficient is reached.

$$mg = \frac{1}{2}\rho V^2 \left[S C_Z + S_h \left(\alpha_{cr} + i_h - \alpha_{cr} \frac{\partial \epsilon}{\partial \alpha} \right) \frac{dC_{Z,h}}{d\alpha} \right] \tag{4.20}$$

Solving this equation for the maximum lift coefficient gives

$$C_{Z,max} = \frac{mg - \frac{1}{2}\rho V_{stall}^2 S_h \left(\alpha_{cr} + i_h - \alpha_{cr} \frac{\partial \epsilon}{\partial \alpha} \right) \frac{dC_{Z,h}}{d\alpha}}{\frac{1}{2}\rho V_{stall}^2 S} \tag{4.21}$$

Assuming that maximum lift coefficient is within linear range, then critical angle of attack is given as follows.

$$C_{Z,max} = C_{Z0} + \alpha_{cr} \frac{dC_Z}{d\alpha} \tag{4.22}$$

Substituting equation (4.22) into (4.21) gives

$$C_{Z0} + \alpha_{cr} \frac{dC_Z}{d\alpha} = \frac{mg - \frac{1}{2}\rho V_{stall}^2 S_h \left(\alpha_{cr} + i_h - \alpha_{cr} \frac{\partial \epsilon}{\partial \alpha} \right) \frac{dC_{Z,h}}{d\alpha}}{\frac{1}{2}\rho V_{stall}^2 S} \tag{4.23}$$

Solving this equation for critical angle of attack gives

$$\alpha_{cr} = \frac{2mg - \rho V_{stall}^2 \left(S_h i_h \frac{dC_{Z,h}}{d\alpha} + S C_{Z0} \right)}{\rho V_{stall}^2 \left[S \frac{dC_Z}{d\alpha} + S_h \left(1 - \frac{\partial \epsilon}{\partial \alpha} \right) \frac{dC_{Z,h}}{d\alpha} \right]} \tag{4.24}$$

4.1.5. XFOIL

XFOIL is a program for the analysis of subsonic isolated airfoils developed at the Massachusetts Institute of Technology. Follow this steps to obtain airfoil characteristics. [32]

1. Execute `xfoil` program.
2. Read buffer airfoil from coordinate file with `LOAD` commad, or set NACA 4 or 5 digit airfoil with `NACA` command e.g. `NACA 2412`.
3. Set number of panels to at least 160 with `PPAR` command.
4. Enter operation mode with `OPER` command. `OPERi` indicates inviscid mode.
5. Enter viscous mode with `Visc` command. Enter Reynolds number for typical flight conditions. `OPERv` should be displayed.
6. Set Mach number for typical flight conditions with `Mach` command.
7. Specify output files with `Pacc` command.
8. Specify the angle of attack range and run computations with `Aseq` command.

4.1.6. VSPAERO

VSPAERO is a combined vortex lattice method (VLM) and panel method solver integrated with OpenVSP, a parametric aircraft geometry tool developed at NASA Ames Research Center. VSPAERO can be used to compute aircraft aerodynamic characteristics within linear range of the lift. [33]

OpenVSP allows users to fast create an aircraft 3D model by defining geometric parameters. An appropriately define aircraft 3D model is needed to analyze. [34] Based on this model degenerated geometry file is generated for the vortex lattice method and surface triangulation file for the panel method.

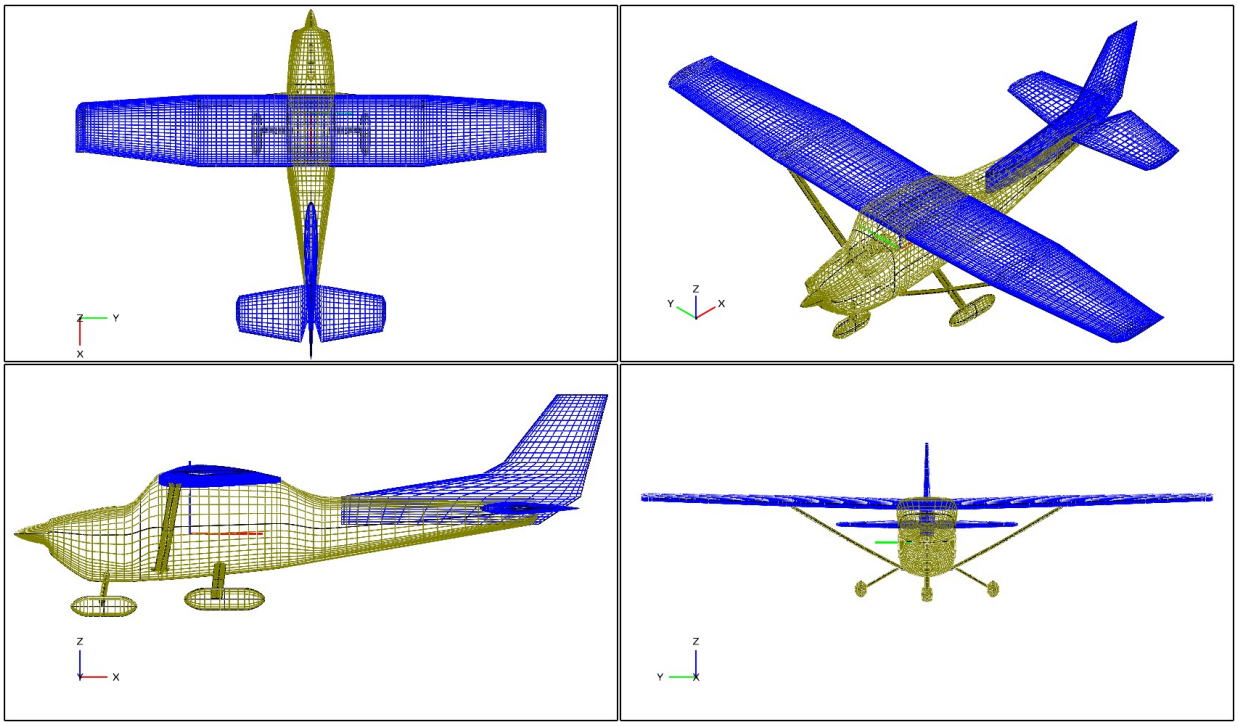

Figure 4-4: OpenVSP aircraft model

VSPAERO can be run from within Analysis menu of the OpenVSP. Some additional setup should be done to start computations. Vortex lattice method or panel method solver should be chosen. Reference area, lengths and moment reference position should be specified to get correct results. Angle of attack range should be specified for the linear range of the lift. Critical angle of attack can be calculated using formula (4.24). Mach number should be set to typical flight conditions.

VSPAERO Viewer and Results Manager can be used to visualize results. Computed aerodynamic characteristics are saved as plain text files, which are both easy to understand by a human and easy to read by a computer program.

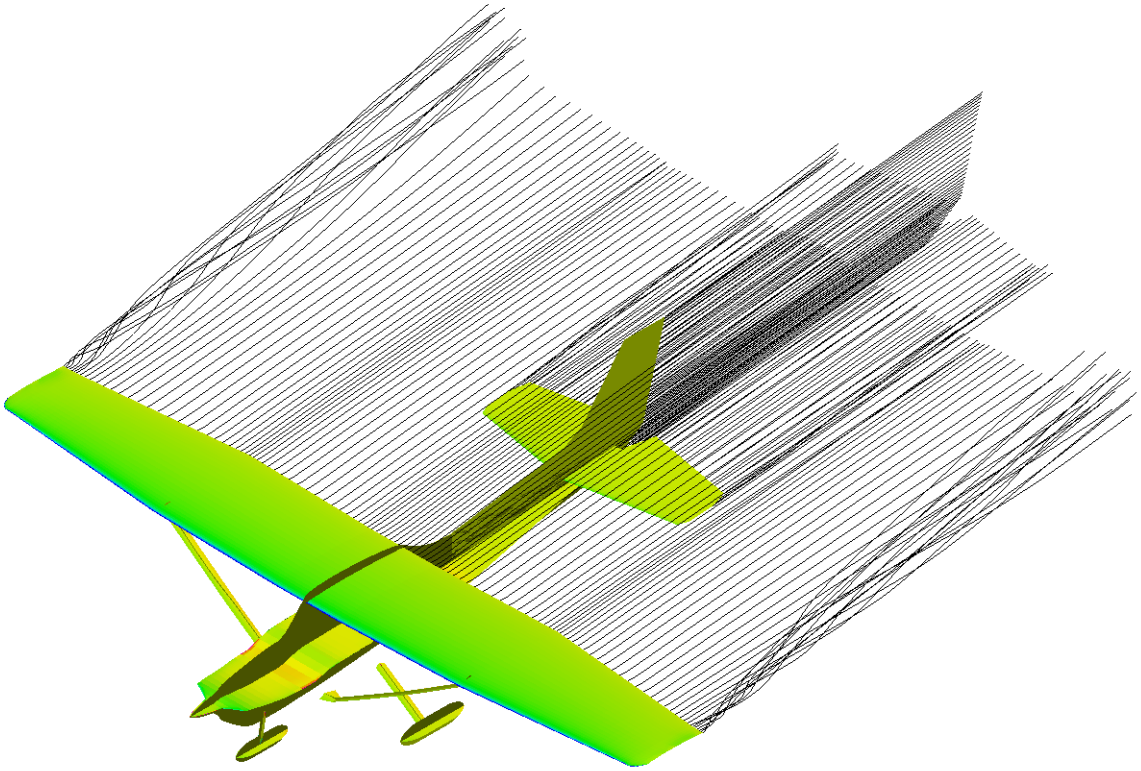

Figure 4-5: Wakes and pressure coefficient change distribution

4.1.7. OpenFOAM

OpenFOAM is an open source software for computational fluid dynamics (CFD) originally created at Imperial College London.

Mesh

OpenFOAM `blockMesh` utility is used to create control volume mesh defined in `system/blockMeshDict` file as a mesh composed of hexahedral blocks. The simplest case is when the control volume is defined by exactly one rectangular prisms.

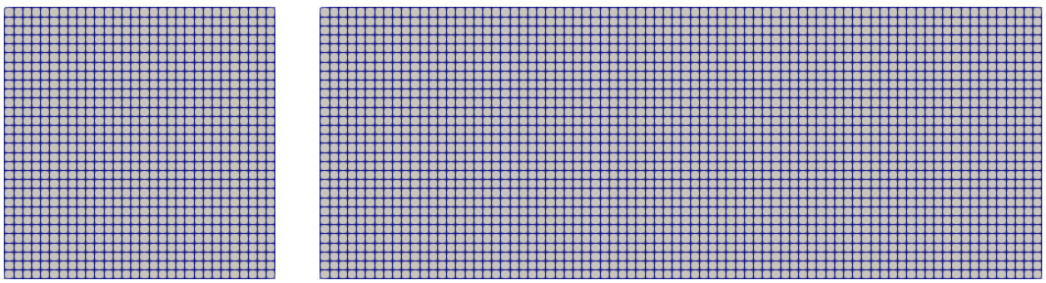

Figure 4-6: Basic control volume mesh

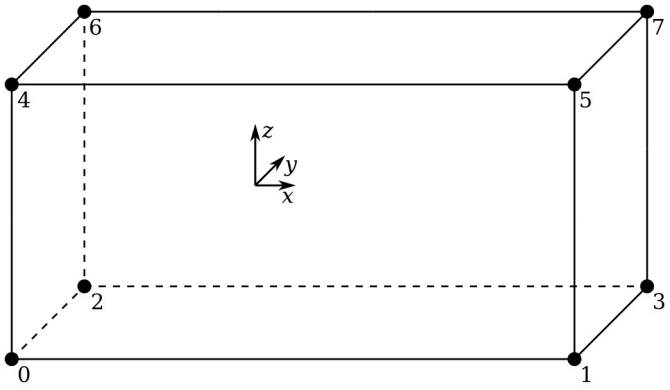

Figure 4-7: Basic control volume scheme

Grading is used to increase mesh resolution in regions of interest.

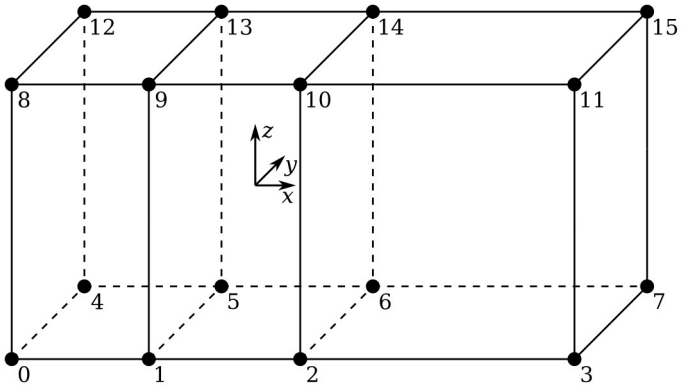

Figure 4-8: Graded control volume scheme

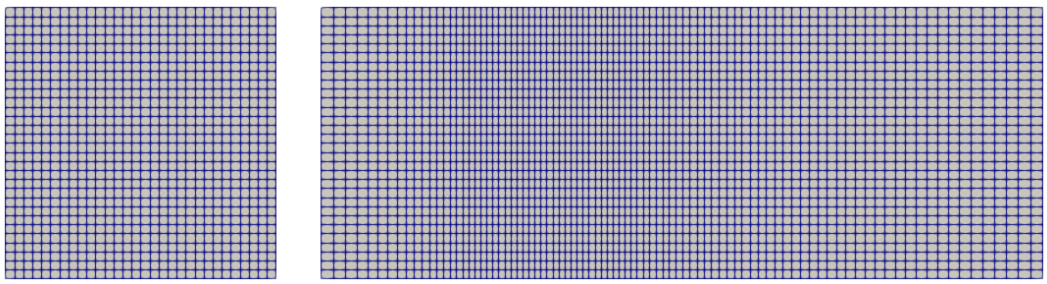

Figure 4-9: Graded control volume mesh

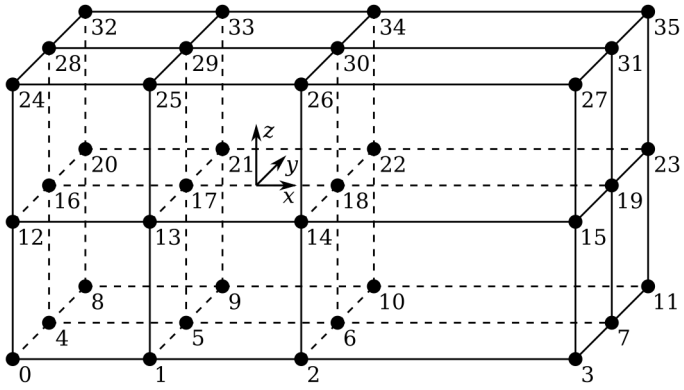

Figure 4-10: Advanced graded control volume scheme

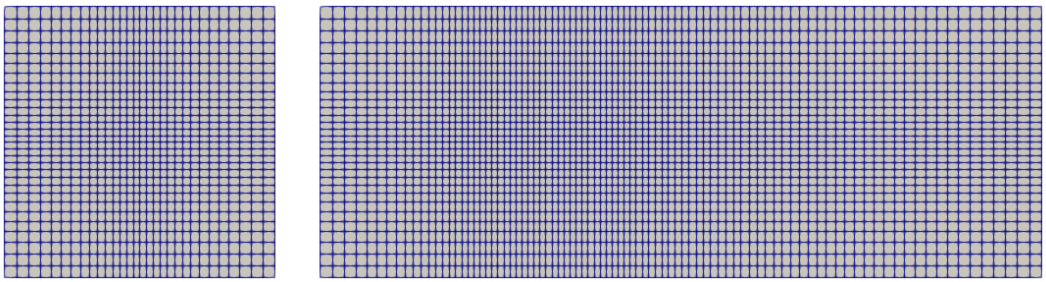

Figure 4-11: Advanced graded control volume mesh

For symmetric cases only half of the geometry can be considered to reduce computation time.

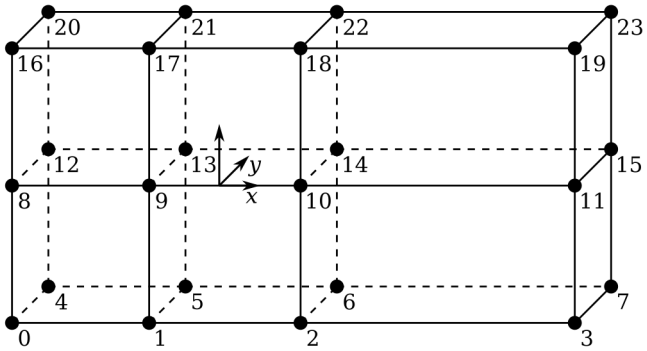

Figure 4-12: Symmetric control volume scheme

OpenFOAM `snappyHexMesh` utility is used to combine control volume mesh with aircraft geometry. `OBJ` or `STL` file can be used to define aircraft geometry. Meshing parameters are specified in `system/snappyHexMeshDict` file.

Mesh refinement is used to increase mesh resolution in regions of interest.

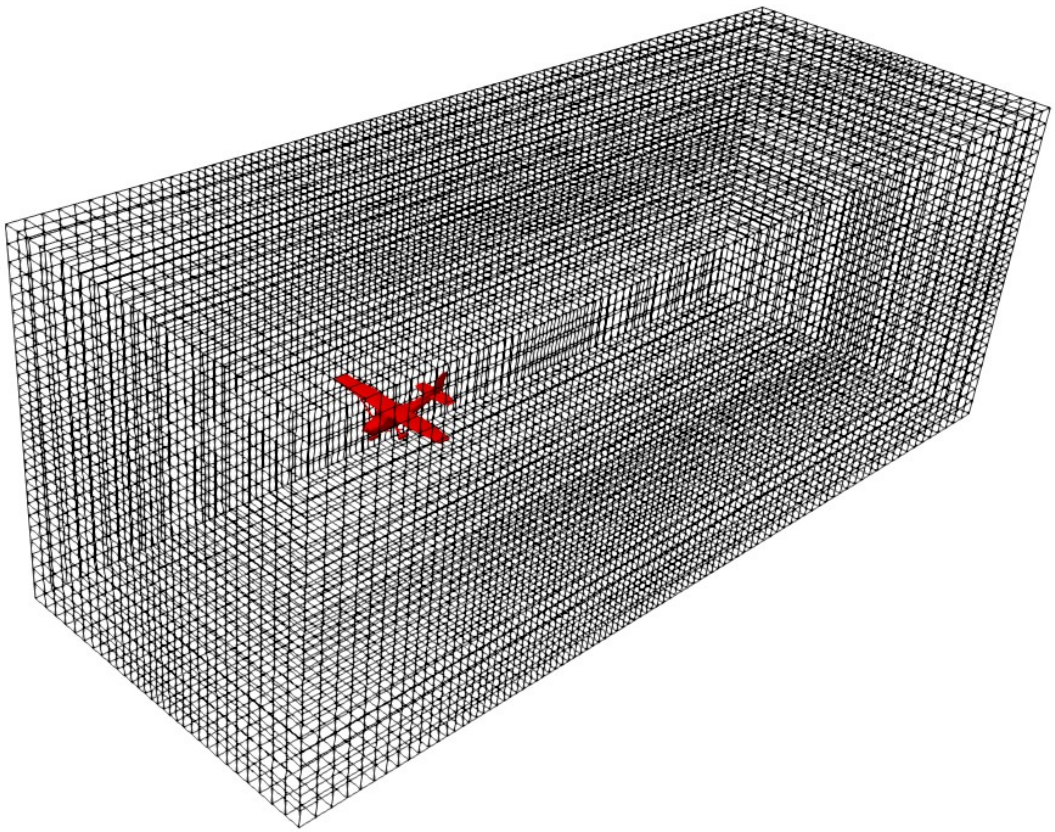

Figure 4-13: Complete mesh

Solver

OpenFOAM `simpleFoam` is a steady-state solver for incompressible, turbulent flow using SIMPLE (Semi-Implicit Method for Pressure Linked Equations) algorithm, which can be used to compute aircraft aerodynamic characteristics for the full range of angle of attack. [35, 36, 37]

SST k-ω Reynolds-Averaged Navier-Stokes (RANS) turbulence model is used.

Initial and Boundary Conditions

The inlet boundary conditions are given as follows. [38]

$$k = \frac{3}{2}(IV)^2 \tag{4.25}$$

$$\omega = \frac{k^{0.5}}{C_\mu L} \tag{4.26}$$

where: [36, 37, 39, 40, 41]

$$I = 0.16\,\mathrm{Re}^{-1/8} \qquad (4.27)$$
$$C_{\mu} = 0.09$$

Control

Notice that, as this is a steady-state simulation, time should be treated rather as iteration parameter rather than as a physical time. Maximum number of iterations in set `system/controlDict` dictionary file, `endTime` is a maximum number of iterations when `deltaT` is 1.

Solution

Case solving is terminated when pressure, velocity, turbulent kinetic energy and specific turbulence dissipation rate initial residual of the field equations falls below threshold values defined in `residualControl` dictionary in `system/fvSolution` file.

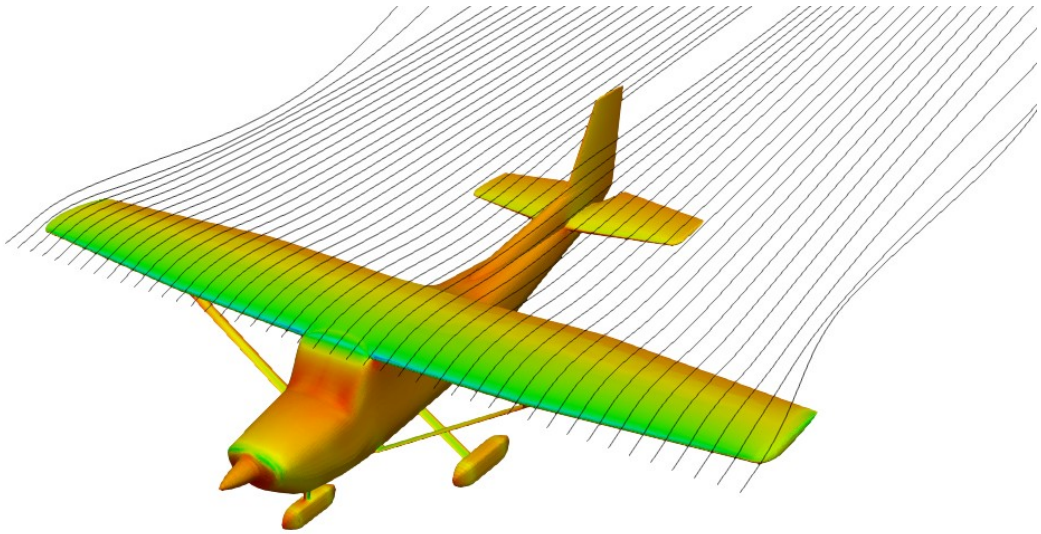

Figure 4-14: Streamlines and kinematic pressure distribution

If divergent or unstable behavior is observed decreasing under-relaxation factors defined in `relaxationFactors` dictionary in `system/fvSolution` file may improve solution convergence.

Physical quantity	Under-Relaxation Factor
Kinematic pressure	0.2 – 0.3
Velocity	0.5 – 0.7
Turbulent kinetic energy	0.5 – 0.7
Turbulence dissipation rate	0.5 – 0.7

Table 4-1: Commonly used under-relaxation factors [41, 42]

4.2. Mass and Inertia Data

4.2.1. Structure Groups Breakdown

Inertia tensor and center of mass coordinates can be estimated by breaking down empty aircraft into structure groups and then estimating their weights, inertia moments and coordinates, e.g. using aircraft drawing. [26]

4.2.2. OpenVSP

Mass Properties tool of the OpenVSP can be used to compute aircraft center of mass position and inertia tensor.

Bibliography

[1] Department of Defense World Geodetic System 1984. National Imagery and Mapping Agency, TR-8350.2, 2000

[2] Padfield G.: Helicopter Flight Dynamics: The Theory and Application of Flying Qualities and Simulation Modelling. Blackwell Publishing, 2007

[3] Sibilski K.: Modelowanie i symulacja dynamiki ruchu obiektów latających. Oficyna Wydawnicza MH, 2004, [in Polish]

[4] Zhu J.: Conversion of Earth-centered Earth-fixed coordinates to geodetic coordinate. IEEE Transactions on Aerospace & Electronic Systems, 1994, No. 30(3), p. 957-961

[5] Taylor J.: Classical Mechanics. University Science Books, 2005

[6] Osiński Z.: Mechanika ogólna. Wydawnictwo Naukowe PWN, 1997, [in Polish]

[7] Leyko J.: Mechanika ogólna. Tom 2: Dynamika. Wydawnictwo Naukowe PWN, 2002, [in Polish]

[8] Allerton D.: Principles of Flight Simulation. John Wiley and Sons, 2009

[9] Stevens B., Lewis F.: Aircraft Control and Simulation. John Wiley and Sons, 1992

[10] Press W., et al.: Numerical Recipes: The Art of Scientific Computing. Cambridge University Press, 2007

[11] Krupowicz A.: Metody numeryczne zagadnień początkowych równań różniczkowych zwyczajnych. Wydawnictwo Naukowe PWN, 1986, [in Polish]

[12] Baron B., Piątek L.: Metody numeryczne w C++ Builder. Helion, 2004, [in Polish]

[13] U.S. Standard Atmosphere 1976. National Oceanic and Atmospheric Administration, National Aeronautics and Space Administration, TM-X-74335, 1976

[14] Flight dynamic - Concepts, quantities and symbols - Part 1: Aircraft motion relative to the air. International Organization for Standardization, ISO 1151-1:1988, 1988

[15] Etkin B.: Dynamics of Atmospheric Flight. John Wiley and Sons, 1972

[16] Gessow A., Myers G.: Aerodynamics of the Helicopter. Frederick Ungar Publishing, 1985

[17] Stepniewski W.: Rotary-Wing Aerodynamics. Volume I: Basic Theories of Rotor Aerodynamics. Dover Publications, 1984

[18] Bramwell A., et al.: Bramwell's Helicopter Dynamics. Butterworth-Heinemann, 2001

[19] Mil M., et al.: Helicopters: Calculation and Design. Volume 1: Aerodynamics. National Aeronautics and Space Administration, TT-F-494, 1967

[20] O'Rourke J.: Computational Geometry in C. Cambridge University Press, 1998

[21] Halliday D., et al.: Fundamentals of Physics. John Wiley and Sons, 2011

[22] Studziński K.: Samochód. Teoria, konstrukcja i obliczanie. Wydawnictwa Komunikacji i Łączności, 1980, [in Polish]

[23] Housner G., Hudson D.: Applied Mechanics: Dynamics. Division of Engineering. California Institute of Technology, 1980

[24] Raymer D.: Aircraft Design: A Conceptual Approach. American Institute of Aeronautics and Astronautics, 1992

[25] Hartman E., Biermann D.: The Aerodynamic Characteristics of Four Full-Scale Propellers Having Different Plan Forms. National Advisory Committee for Aeronautics, TR-643, 1938

[26] Torenbeek E.: Synthesis of Subsonic Airplane Design. Delft University Press, 1982

[27] Kaczorek T., et al.: Podstawy teorii sterowania. Wydanie drugie zmienione. Wydawnictwo Naukowo-Techniczne, 2006, [in Polish]

[28] Skup Z.: Podstawy automatyki i sterowania. Politechnika Warszawska, 2012, [in Polish]

[29] Takahashi M.: A Flight-Dynamic Helicopter Mathematical Model with a Single Flap-Lag-Torsion Main Rotor. National Aeronautics and Space Administration, TM-102267, 1990

[30] Critzos C., et al.: Aerodynamic Characteristics of NACA 0012 Airfoil Sections at Angles of Attack from 0 to 180. National Advisory Committee for Aeronautics, TN-3361, 1955

[31] Sheldahl R., Klimas P.: Aerodynamic Characteristics of Seven Symmetrical Airfoil Sections Through 180-Degree Angle of Attack for Use in Aerodynamic Analysis of Vertical Axis Wind Turbines. Sandia National Laboratories, 1981

[32] Drela M., Youngren H.: XFOIL 6.9 User Primer. [online]. 2001 [Accessed 2019-01-20]. Available from: https://web.mit.edu/drela/Public/web/xfoil/xfoil_doc.txt

[33] Litherland B.: Using VSPAERO. [online]. 2015 [Accessed 2019-01-20]. Available from: http://openvsp.org/wiki/doku.php?id=vspaerotutorial

[34] Litherland B.: Modeling for VSPAERO. [online]. 2015 [Accessed 2019-05-12]. Available from: http://openvsp.org/wiki/doku.php?id=vspaeromodeling

[35] Greenshields C.: OpenFOAM User Guide version 6. OpenFOAM Foundation Ltd., 2018

[36] Moukalled F., Mangani L., Darwish M.: The Finite Volume Method in Computational Fluid Dynamics, An Advanced Introduction with OpenFOAM and Matlab. Springer International Publishing, 2016

[37] Versteeg H., Malalasekera W.: An Introduction to Computational Fluid Dynamics, The Finite Volume Method. Pearson Education Limited, 2007

[38] OpenFOAM: User Guide: k-omega Shear Stress Transport (SST). [online]. 2019 [Accessed 2019-05-19]. Available from: https://www.openfoam.com/documentation/guides/latest/doc/guide-turbulence-ras-k-omega-sst.html

[39] Andersson B., et. al.: Computational Fluid Dynamics for Engineers. Cambridge University Press, 2012

[40] Ferziger J., Perić M.: Computational Methods for Fluid Dynamics. Springer-Verlag, 2002

[41] ANSYS Fluent User's Guide, Release 15.0. ANSYS, Inc., 2013

[42] Guerrero J.: Tips and tricks in OpenFOAM®. [online]. 2018 [Accessed 2019-05-19]. Available from: http://www.wolfdynamics.com/wiki/OFtipsandtricks.pdf